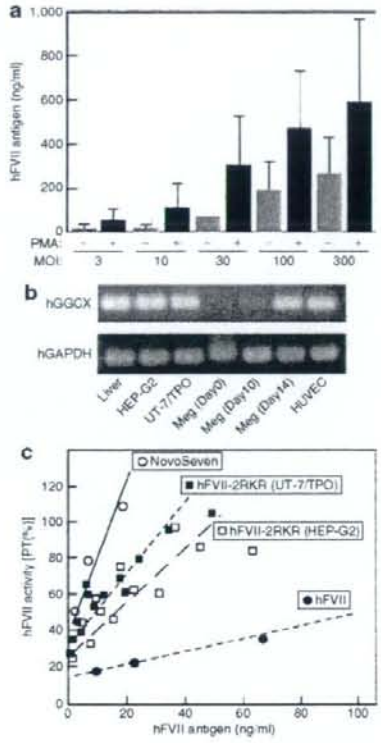

Figure 3 Production of functional hFVII-2RKR by UT-7/TPO cells transduced with simian immunodeficiency virus (SIV) vector. (**a**) UT-7/TPO cells were transduced with SIV-CMV-hFVII-2RKR at the multiplicity of infection (MOI) indicated. hFVII antigen in the supernatant from the cells treated without or with 5 μmol/l phorbol 12-myristate 13-acetate (PMA) for 24 hours were measured using enzyme-linked immunosorbent assay. Columns and error bars represent the mean ± SD ($n = 3$). (**b**) mRNA expression of γ-glutamyl carboxylase (GGCX) was determined using reverse transcriptase-PCR (RT-PCR). As a control, RT-PCR analysis for human glyceraldehyde 3-phosphate dehydrogenase (GAPDH) transcript was performed simultaneously. (**c**) Comparison between activity and antigen levels of hFVII-2RKR produced by UT-7/TPO and HEP-G2 cells, NovoSeven, and plasma-derived full-length hFVII. CMV, cytomegalovirus; hFVII, human factor VII; HUVEC, human umbilical vein endothelial cells; Meg, CD34$^+$-derived megakaryocytes at days 0, 10, and 14 after the start of differentiation with 10 ng/ml of interleukin-3 and 50 ng/ml of thrombopoietin.

factor, was confirmed in megakaryocytes (Figure 3b). These data suggest that platelet precursor megakaryocytes efficiently produce functional FVIIa after transduction.

We next examined whether transduction of HSCs enabled FVIIa expression in platelets. For this purpose, hFVII was used to discriminate transduced FVII from endogenous mFVII. An SIV vector equipped with *hFVII-2RKR* driven by *GPIbα* promoter was created (Figure 2b) and used for infecting unfractionated bone marrow cells. After transplantation of the transduced cells into lethally irradiated FVIII-deficient mice, hFVII antigen levels were detected in platelet lysates for at least 90 days (Figure 4a). Importantly, hFVII antigen was not detected in the plasma even after stimulation of the

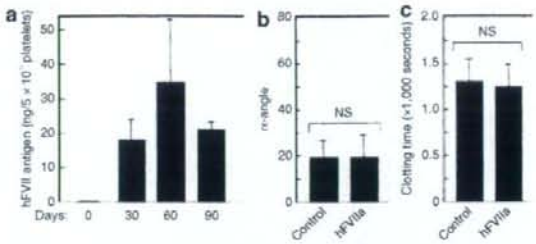

Figure 4 Human factor VII (hFVII) expression in platelets after transplantation of transduced stem cells. FVIII-deficient mice were given transplants of unfractionated bone marrow cells transduced without (control) or with SIV-GPIbα-hFVII-2RKR (hFVIIa). (**a**) Peripheral blood was drawn from the transplant-recipient mice at the indicated times, and the hFVII antigen levels in platelet lysates were measured using enzyme-linked immunosorbent assay. Columns and error bars represent the mean ± SD ($n = 4$ per group). (**b** and **c**) Whole-blood coagulation was assessed using thromboelastography. Quantitative data of panel **b** α-angle and panel **c** clotting time are shown ($n = 7$ for control; $n = 8$ for hFVIIa). Columns and error bars represent the mean ± SEM. Differences between the two groups were analyzed statistically using Student's *t*-test. NS, not significant. SIV, simian immunodeficiency virus.

platelets with collagen and phorbol 12-myristate 13-acetate (data not shown); therefore, we did not assay for FVII activity in plasma.

We next examined the improvement of whole-blood coagulation in the transplant-recipient mice. The conventional activated partial thromboplastin time, a useful marker for gene therapy in mouse models of hemophilia, did not seem to reflect the phenotypic correction directly, as seen from the fact that platelet-derived hFVII antigen could not be detected in plasma. Therefore we employed thromboelastography (TEG) to record the continuous profile of whole-blood coagulation.[10] TEG can be used for evaluating the effects of hemostatic agents such as rhFVIIa,[11] and to assess the effects of different pharmacological interventions on various factors (coagulation, platelet activation, and platelet–fibrin interaction) involved in clot formation. As shown in Figure 4b and c, whole-blood coagulation in FVIII-deficient mice, as assessed by TEG, did not improve after transplantation. The mortality rate after tail clipping was not altered by transplantation (data not shown).

In order to investigate why phenotypic correction was not observed after transplantation, we validated the expression and localization of hFVII by immunogold electron microscopy. We confirmed that hFVII antigen was abundant in cytoplasm of platelets obtained from transplant-recipient mice (Figure 5a). When platelets were stimulated with phorbol 12-myristate 13-acetate, most of the hFVII antigen was redistributed to the sub-membrane zone, and was partly expressed on the surface (Figure 5b). These data confirmed that hFVII is efficiently stored in platelets after transplantation of transduced bone marrow cells, and is expressed on the cell surface after platelet activation.

Phenotype correction of FVIII-deficient mice by expression of mFVII-2RKR in platelets

We hypothesized that the failure of hFVII-2RKR expression in platelets may be because of inefficient interaction of hFVII-2RKR with murine TF.[12,13] Indeed, higher concentrations of rhFVIIa (NovoSeven; ≥20 μg/ml) were required to restore coagulation in

FVIII-deficient mice (data not shown). We therefore generated an mFVII construct in an analogous fashion (mFVII-2RKR) to further prove its efficacy in FVIII-deficient mice (Figure 2b). Because we could not create an enzyme-linked immunosorbent assay for mFVII antigen, an *eGFP* gene driven by the internal ribosomal entry site was inserted just after the *mFVII-2RKR* gene to give indirect confirmation of mFVII-2RKR expression in platelets (Figure 2b). Although eGFP expression in platelets after transplantation was limited to 3–12% of the platelets, the pattern of eGFP expression under the control of the internal ribosomal entry site sequence was much weaker than that driven directly by the upstream promoter (data not shown). It appears, therefore, that the levels of ectopically expressed mFVII-2RKR in platelets are much higher than would be expected from the results of eGFP expression. This reasoning was supported by the results of proviral integration into the genome (1.15 ± 2.42; $n = 13$), which were similar to those obtained from mice expressing eGFP in 28.6–74.3% of platelets by transduction with SIV-GPIbα-eGFP (see Figure 1c).

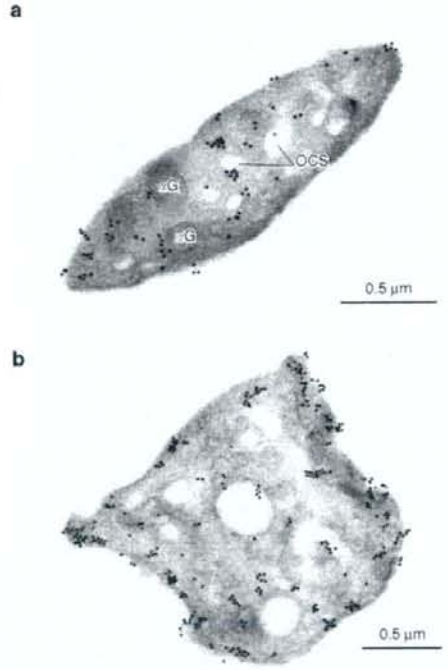

Figure 5 Immunoelectron microscopic localization of ectopically expressed hFVII-2RKR in platelets. FVIII-deficient mice were given transplants of unfractionated bone marrow cells transduced with SIV-GPIbα-hFVII-2RKR. Isolated platelets from the transplant-recipient mice were stimulated (**a**) without or (**b**) with 100 nmol/l phorbol 12-myristate 13-acetate for 15 minutes. Cells were incubated with a biotin-labeled rabbit anti-hFVII antibody. Bound antibodies were detected using a colloidal gold–conjugated goat anti-biotin secondary antibody. hFVII expression in platelets was examined by electron microscopy. αG, α-granule; hFVII, human factor VII; OCS, open canalicular system; SIV, simian immunodeficiency virus.

In comparison with the results obtained from hFVII-2RKR, whole-blood coagulation, as assessed by TEG, was significantly improved in mice that had received the transplant (Figure 6a). The α-angle, which represents the rate of clot formation, was enhanced (Figure 6b), and the clotting time was significantly shortened

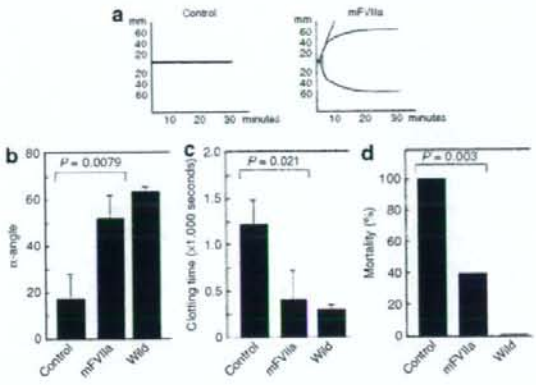

Figure 6 Phenotype correction of factor VIII (FVIII)-deficient mice by ectopic expression of mFVII-2RKR in platelets. FVIII-deficient mice were given transplants of unfractionated bone marrow cells transduced without (control) or with SIV-GPIbα-mFVII-2RKR (mFVIIa). (**a**) Representative thromboelastography data obtained from control and mFVII-2RKR-transfected mice. (**b** and **c**) Quantitative data of panel **b** α-angle and panel **c** clotting time are shown ($n = 8$ for control; $n = 8$ for mFVIIa). The data obtained from wild-type mice are also shown ($n = 6$). Columns and error bars represent the mean ± SEM. Differences between the two groups were analyzed statistically using Student's *t*-test. (**d**) Mortality rates within 24 hours of tail clipping in wild-type mice ($n = 6$) or FVIII-deficient mice given transplants of control or SIV-GPIbα-mFVII-2RKR-transduced bone marrow cells ($n = 10$ for control; $n = 10$ for mFVIIa). The mortality rate was analyzed statistically using the χ^2-test. mFVIIa, murine activated factor VII; SIV, simian immunodeficiency virus.

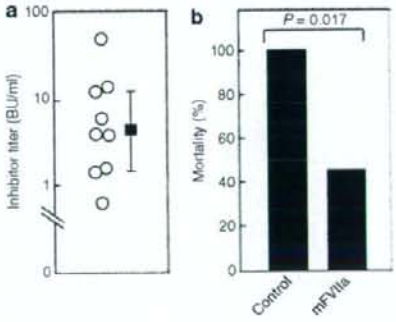

Figure 7 Effects of mFVII-2RKR expression in platelets on phenotypic correction in factor VIII (FVIII)-deficient mice in the presence of anti-FVIII inhibitors. (**a**) Circulating inhibitors were detected in 9 of the 13 FVIII-deficient mice after peritoneal injection of recombinant hFVIII. (**b**) In the presence of circulating inhibitors, mortality ratio at 24 hours after tail clipping was examined in FVIII-deficient mice given transplants of control or SIV-GPIbα-mFVII-2RKR-transduced bone marrow cells [$n = 10$ for control; $n = 9$ for mFVII-2RKR (mFVIIa)]. The mortality rate was analyzed statistically using the χ^2-test. mFVIIa, murine activated factor VII; SIV, simian immunodeficiency virus.

(Figure 6c). The mortality rate after tail clipping was significantly reduced in mice with transplants (Figure 6d). In addition, five of the nine FVIII-deficient mice that received bone marrow cells transduced with SIV-GPIbα-mFVII-2RKR survived after tail clipping despite the presence of circulating inhibitors against hFVIII (Figure 7a and b). Blood coagulation, as assessed by TEG, was similarly corrected in FVIII-deficient mice having FVIII-neutralizing inhibitors, by treating them with SIV-GPIbα-mFVII-2RKR (data not shown). Taking these results together, platelet-specific mFVII-2RKR expression results in efficient bypass therapy to activate factor X activation, thereby resulting in thrombin generation on platelet surfaces in FVIII-deficient mice.

DISCUSSION

Hemophilia is considered to be a suitable condition for gene therapy because it is caused by a single gene abnormality, and therapeutic coagulation factor levels may vary across a broad range (5–100%).[11] Although sustained therapeutic expression of FVIII has been achieved in preclinical studies using a wide range of gene transfer technologies targeted at different tissues, the emergence of neutralizing antibodies often limits the clinical applications.[13] Blood platelets have been receiving much attention as novel target cells for hemophilia gene therapy, because platelet-specific expression of FVIII abolishes the emergence of neutralizing antibodies, and platelet-derived FVIII supports hemostasis in the presence of high titers of FVIII-neutralizing antibodies.[2–5] Here, we extended the application of platelet-directed gene therapy to demonstrate that FVII-2RKR expression in platelets improved the bleeding phenotype of FVIII-deficient mice, even in the presence of FVIII-neutralizing antibodies. Given that rhFVIIa has proven efficacy in the treatment of hemophilia patients with the inhibitors,[8] platelets expressing FVII-2RKR may be a potential alternative to bolus administration of rhFVIIa in such patients.

It is possible that platelets store ectopically expressed FVII-2RKR in the cytoplasm, and that this is specifically expressed on the cell surface after activation. Although hFVII antigen levels achieved here seemed to be much lower than the therapeutic level, whole-blood clotting, as assessed by TEG, and mortality rate after tail clipping were significantly improved when mFVII-2RKR was expressed. These data suggest that FVII-2RKR in platelets can locally generate a thrombin burst at the site of vascular injury. Although an important drawback of rhFVIIa administration is its short half-life (2.6–2.8 hours), which necessitates frequent bolus injections to stop bleeding,[7,16] platelets may be able to store stable FVII-2RKR in the circulation. The importance of coagulation factor stored in platelets is supported by the role of platelet factor V in hemostasis. Platelet-derived platelet factor V appears to support hemostasis even in patients with an acquired platelet factor V inhibitor, thereby suggesting that platelets can deliver coagulation factors and protect them from being degraded by platelet factor V inhibitors.[17] Recently, erythroid-specific factor IX expression, driven by the *β-globin* promoter, has been shown to result in phenotypic correction of hemophilia B in mice.[18] However, given the context of the specific release or expression of a target protein at the site of thrombus formation, platelet-directed gene therapy has an advantage as a therapy for inherited coagulation factor deficiencies.

Contrary to our initial expectations, the sub-localization of ectopically expressed hFVII-2RKR in platelets is quite different from that described in previous reports of FVIII expression.[3,19] Retroviral transduction of FVIII in human $CD34^+$ HSCs enables FVIII-transduced megakaryocytes to store human FVIII with von Willebrand factor, a natural carrier protein of FVIII, within α-granules.[19] In this study, hFVII-2RKR was found to be localized in the cytoplasm, but not in α-granules, suggesting that storage of this ectopically expressed protein in α-granules requires specific binding with an endogenous protein, as is the case for the FVIII–von Willebrand factor interaction.[20] Despite the failure to localize in α-granules, cytoplasmic hFVII-2RKR translocated to a sub-membrane fraction and was expressed on the cell surface after platelet activation. It is possible that activated platelets can express FVII-2RKR through a mechanism of protein secretion other than granule release. Phosphatidylserine flip-flop is one candidate that may be responsible for the surface expression of FVII-2RKR; however, we do not yet have a clear explanation for this. Recently, it has been reported that platelets supply their own TF for thrombin generation in a temporally and spatially circumscribed process.[21,22] This would suggest that TF expression in platelets is involved in the hemostatic function of ectopically expressed FVII-2RKR, even in the absence of soluble TF. The failure of hFVII-2RKR expression in platelets to correct the bleeding phenotype, in contrast to mFVII-2RKR, further demonstrates the TF-dependence of coagulation mediated by platelet-derived FVIIa; murine TF appears to be more species-specific and interacts poorly with hFVIIa.[12,13]

Before proceeding to further clinical application, we should weigh the clinical benefits and risks of FVII-2RKR expression in platelets. The most important drawback of FVIIa expression is a potential risk for thromboembolic events. In this study, the clinical effect of FVII-2RKR expression seemed to be less than that of FVIII expression in platelets. Although a correction of as little as 1% of FVIII in platelets was reportedly enough to cure FVIII-null mice,[3–5] our strategy resulted only in a partial cure in the current model. One explanation of the lower efficacy is that much higher expression of FVII-2RKR is needed to generate sufficient thrombin in FVIII-deficient mice. We will need to further improve the transduction efficiency and modify the enzymatic activity of FVIIa. We believe that megakaryocyte- and platelet-specific expression of FVIIa in targeting HSCs is important for safety, given that expression of FVIIa in neutrophils or monocytes may alter the coagulation properties of blood cells, leading to an unexpected thrombosis similar to disseminated intravascular coagulation. Once the approach involving the targeting of platelets has been optimized for greater efficacy, it is possible that the risk of unexpected thrombosis will become a major concern. Further, we must consider the risk of insertional mutagenesis of the integrating vector. While lentiviral vectors offer a means to correct genetic diseases by integration into chromosomal DNA permanently, all the integrating gene transfer vectors in current use carry a risk of insertional mutagenesis.[23] In view of the fact that the target diseases for platelet-directed gene therapy, including hemophilia, are not generally lethal disorders, we have to continue investigating the safety of platelet-directed gene therapy using integrating vectors to the maximum. Observations should be carried on for extended durations in order

to substantiate long-term *in vivo* gene expression and vector safety. Our observations were limited to 3 months.

In this study, we demonstrated that FVII-2RKR expression in platelets by SIV vectors could be an important strategy for treating hemophilia A. Given that platelets play a central role and provide the scaffolding for the coagulation cascade, this would be a reasonable approach, similar to the proven therapeutic effects of rhFVIIa infusion, for treating a number of hemorrhagic diseases, such as hemophilia, Glanzmann's thrombasthenia, and FVII deficiency. Further evaluations utilizing larger animals such as Cynomolgus monkeys or dogs will be necessary to determine efficient and safe protocols for platelet-directed gene therapy.

MATERIALS AND METHODS

The materials and methods for cell culture, reverse transcriptase-PCR, proviral integration, mouse blood preparation, enzyme-linked immunosorbent assay for hFVII antigen, determination of hFVII activity, and flow cytometry are described in the **Supplementary Materials and Methods**.

Plasmid constructs and production of SIV lentiviruses. The methods for cDNA cloning and plasmid construction are described in detail in **Supplementary Materials and Methods**. A self-inactivating SIV vector plasmid was generated as described earlier (Figure 1b).[24] SIV lentiviral vectors were produced as described earlier.[4] Briefly, the SIV vector and each packaging vector (*gag/pol*, *rev*, and *VSV-G*) were co-transfected into HEK293T cells using the Lipofectamine PLUS reagent (Invitrogen, Carlsbad, CA). The supernatants were collected 48 hours after transfection and filtered through a 0.4-μm filter. The transduction units of the lentiviral vector and proviral integration into the genomic DNA were measured as described earlier.[4]

Isolation of KSL cells, viral transduction, and stem cell transplantation. Mice with FVIII-deficient hemophilia A with targeted destruction of exon 16 of the *FVIII* gene were kindly provided by Dr H.H. Kazazian Jr. (University of Pennsylvania, Philadelphia, PA). C57BL/6 (Ly5.2) mice were purchased from Japan SLC (Shizuoka, Japan). C57BL/6 mice congenic for the Ly5 locus (Ly5.1) were purchased from Sankyo-Lab Service (Tokyo, Japan). All animal procedures were approved by the Institutional Animal Care and Concern Committee at Jichi Medical University (Tochigi, Japan), and animal care was in accordance with the committee's guidelines.

KSL HSCs were isolated as described earlier.[4] KSL cells or unfractionated bone marrow cells were precultured for 24 hours before viral transduction in Stem Pro Medium (Invitrogen, Carlsbad, CA) supplemented with 100 ng/ml stem cell factor, 10 ng/ml thrombopoietin, 100 ng/ml interleukin-6, 100 ng/ml Flt-3 ligand, and 400 ng/ml soluble interleukin-6 receptor. The cells were transduced with SIV vectors at a multiplicity of infection of 30 in the presence of the same cytokine combination, and incubated at 37 °C for 12 hours. The recipient mice (Ly5.2 mice or FVIII-deficient mice at 8–12 weeks of age) were irradiated with a single lethal dose of 9.5 Gy (Gamma Cell; Norton International, Ontario, Canada), and then administered either transduced KSL cells (1×10^4) and Ly5.2 competitor cells (2×10^5), or transduced whole bone marrow cells (2×10^6). The methods for transduction of UT-7/TPO and HEP-G2 cells by SIV vector are described in **Supplementary Materials and Methods**.

Immunogold electron microscopy. Washed murine platelets were obtained as described earlier.[25] The resting and phorbol 12-myristate 13-acetate-stimulated platelets were fixed in 0.1% glutaraldehyde in 0.1 mol/l phosphate buffer (pH 7.4) at 4 °C for 1 hour. The fixed platelets were transferred into Eppendorf tubes, centrifuged at 3,000 rpm for 3 minutes, and rinsed with phosphate-buffered saline five times at 4 °C. The specimens were sequentially immersed in 1 mol/l sucrose in phosphate-buffered saline for 1 hour, and then in 1.84 mol/l sucrose containing 20% polyvinylpyrrolidone (Sigma-Aldrich, St. Louis, MO) in phosphate-buffered saline overnight at 4 °C.[26] The specimens were frozen in liquid nitrogen and ultra-thin frozen sections were prepared, incubated with biotin-labeled rabbit anti-hFVII antibody, washed with phosphate-buffered saline, and then incubated with goat anti-biotin antibody coupled to 15 colloidal gold (BBI International, Cardiff, UK). After being stained with uranyl acetate, the sections were examined using a JEM-1200EX electron microscope (JEOL, Tokyo, Japan) at an acceleration voltage of 80 kV.

TEG and tail clipping. The principle of TEG is based on measurement of the physical viscoelastic characteristics of blood clots. Whole blood for TEG was drawn at 30–60 days after transplantation. Clot formation was monitored in whole blood at 37 °C, in an oscillating plastic cylindrical cuvette having a coaxially suspended stationary piston with 1-mm clearance between the surfaces, using a computerized TEG (ROTEG; Pentapharm, Munich, Germany). A sample (270 μl) of whole blood was carefully drawn from the superior vena cava of anesthetized mice using a syringe containing 30 μl sodium citrate. Whole-blood coagulation was initiated with the addition of 20 μl of 200 mmol/l $CaCl_2$, and TEG was used to assess the coagulation by measuring various parameters, such as the latency for clotting time, and the kinetics of clot development, as determined by the α-angle.[18] When blood coagulation was not observed within 30 minutes, the clotting time and α-angle were defined as 1,800 seconds and 0°, respectively. Phenotypic correction was tested in some of the transplant-recipient mice by anesthetizing them with diethyl ether and clipping 1.0 cm off the ends of their tails. The mice were then observed for 24 hours to determine the rate of mortality.

Circulating FVIII inhibitors. Antibodies against hFVIII were produced by administering weekly peritoneal injections of 0.05 U/g body weight of rhFVIII (Kogenate FS; Bayer AG, Wuppertal, Germany). In view of the possibility that lethal irradiation could cancel the circulating anti-FVIII antibodies (data not shown), we started immunization with hFVIII 1 month after transplantating bone marrow cells transduced with SIV-GPIbα-mFVII-2RKR. Analysis of neutralizing antibodies against hFVIII was performed using the Bethesda method described earlier.[27] After five immunizations, we could detect circulating inhibitors against hFVIII, as assessed in Bethesda units (Figure 7a).

SUPPLEMENTARY MATERIAL

Materials and Methods.

ACKNOWLEDGMENTS

We are deeply grateful to Naoko Matsumoto and Masanori Ito for their excellent technical assistance. We are also grateful to H.H. Kazazian Jr. (University of Pennsylvania, Philadelphia, PA) for providing the FVIII-deficient mice, and N. Komatsu (Yamanashi University, Yamanashi, Japan) for UT-7/TPO. This work was supported by grants from the Mitsubishi Pharma Research Foundation (to T.O.), Grants-in-aid for Scientific Research from the Ministry of Education and Science (19591133 to S.M. and 18591084 to J.M.), Health and Labour Science Research Grants for Research from the Ministry of Health, Labour and Welfare (H17-nanchi-ippan-002 and H18-eizu-ippan-003 to Y.S.), and grants for "High-Tech Center Research" Projects for Private Universities with matching fund subsidies from MEXT (Ministry of Education, Culture, Sports, Science and Technology), 2002–2006 (to Y.S).

REFERENCES

1. Kuter, D, Eslin, DE, Bdeir, K, Murciano, JC, Kuo, A, Kowalska, MA *et al.* (2003). Antithrombotic thrombocytes: ectopic expression of urokinase-type plasminogen activator in platelets. *Blood* **102**: 926–933.
2. Yarovoi, HV, Kuter, D, Eslin, DE, Thornton, MA, Haberichter, SL, Shi, Q *et al.* (2003). Factor VIII ectopically expressed in platelets: efficacy in hemophilia A treatment. *Blood* **102**: 4006–4013.
3. Shi, Q, Wilcox, DA, Fahs, SA, Weiler, H, Wells, CW, Cooley, BC *et al.* (2006). Factor VIII ectopically targeted to platelets is therapeutic in hemophilia A with high-titer inhibitory antibodies. *J Clin Invest* **116**: 1974–1982.
4. Ohmori, T, Mimuro, J, Takano, K, Madoiwa, S, Kashiwakura, Y, Ishiwata, A, *et al.* (2006). Efficient expression of a transgene in platelets using simian immunodeficiency

virus-based vector harboring glycoprotein Ibalpha promoter: in vivo model for platelet-targeting gene therapy. *FASEB J* **20**: 1522–1524.
5. Shi, Q, Wilcox, DA, Fahs, SA, Tang, J, Johnson, BD, Du, LM *et al.* (2007). Lentivirus-mediated platelet-derived factor VIII gene therapy in murine haemophilia A. *J Thromb Haemost* **5**: 352–361.
6. Mackman, N, Tilley, RE and Key, NS (2007). Role of the extrinsic pathway of blood coagulation in hemostasis and thrombosis. *Arterioscler Thromb Vasc Biol* **27**: 1687–1693.
7. Jurlander, B, Thim, L, Klausen, NK, Persson, E, Kjalke, M, Rexen, P *et al.* (2001). Recombinant activated factor VII (rFVIIa): characterization, manufacturing, and clinical development. *Semin Thromb Hemost* **27**: 373–384.
8. Franchini, M, Zaffanello, M and Veneri, D (2005). Recombinant factor VIIa. An update on its clinical use. *Thromb Haemost* **93**: 1027–1035.
9. Margaritis, P, Arruda, VR, Aljamali, M, Camire, RM, Schlachterman, A and High, KA (2004). Novel therapeutic approach for hemophilia using gene delivery of an engineered secreted activated factor VII. *J Clin Invest* **113**: 1025–1031.
10. Luddington, RJ (2005). Thrombelastography/thromboelastometry. *Clin Lab Haematol* **27**: 81–90.
11. Sørensen, B and Ingerslev, J (2004). Thromboelastography and recombinant factor VIIa-hemophilia and beyond. *Semin Hematol* **41(suppl. 1)**: 140–144.
12. Janson, TL, Stormorken, H and Prydz, H (1984). Species specificity of tissue thromboplastin. *Haemostasis* **14**: 440–444.
13. Nelsestuen, GL, Stone, M, Martinez, MB, Harvey, SB, Foster, D and Kisiel, W (2001). Elevated function of blood clotting factor VIIa mutants that have enhanced affinity for membranes. Behavior in a diffusion-limited reaction. *J Biol Chem* **276**: 39825–39831.
14. Lozier, J (2004). Gene therapy of the hemophilias. *Semin Hematol* **41**: 287–296.
15. High, K (2005). Gene transfer for hemophilia: can therapeutic efficacy in large animals be safely translated to patients? *J Thromb Haemost* **3**: 1682–1691.
16. Hedner, U (2001). Recombinant factor VIIa (Novoseven) as a hemostatic agent. *Semin Hematol* **38**(suppl. 12): 43–47.
17. Perdekamp, MT, Rubenstein, DA, Jesty, J and Hultin, MB (2006). Platelet factor V supports hemostasis in a patient with an acquired factor V inhibitor, as shown by prothrombinase and tenase assays. *Blood Coagul Fibrinolysis* **17**: 593–597.
18. Chang, AH, Stephan, MT and Sadelain, M (2006). Stem cell-derived erythroid cells mediate long-term systemic protein delivery. *Nat Biotechnol* **24**: 1017–1021.
19. Wilcox, DA, Shi, Q, Nurden, P, Haberichter, SL, Rosenberg, JB, Johnson, BD *et al.* (2003). Induction of megakaryocytes to synthesize and store a releasable pool of human factor VIII. *J Thromb Haemost* **1**: 2477–2489.
20. Federici, AB (2003). The factor VIII/von Willebrand factor complex: basic and clinical issues. *Haematologica* **88**: EREP02.
21. Panes, O, Matus, V, Saez, CG, Quiroga, T, Pereira, J and Mezzano, D (2007). Human platelets synthesize and express functional tissue factor. *Blood* **109**: 5242–5250.
22. Schwertz, H, Tolley, ND, Foulks, JM, Denis, MM, Risenmay, BW, Buerke, M *et al.* (2006). Signal-dependent splicing of tissue factor pre-mRNA modulates the thrombogenicity of human platelets. *J Exp Med* **203**: 2433–2440.
23. Nienhuis, AW, Dunbar, CE and Sorrentino, BP (2006). Genotoxicity of retroviral integration in hematopoietic cells. *Mol Ther* **13**: 1031–1049.
24. Nakajima, I, Nakamaru, K, Ido, E, Terao, K, Hayami, M and Hasegawa, M (2000). Development of novel simian immunodeficiency virus vectors carrying a dual gene expression system. *Hum Gene Ther* **11**: 1863–1874.
25. Leng, XH, Hong, SY, Lamucea, S, Zhang, W, Li, TT, López, JA *et al.* (2004). Platelets of female mice are intrinsically more sensitive to agonists than are platelets of males. *Arterioscler Thromb Vasc Biol* **24**: 376–381.
26. Suzuki, H, Murasaki, K, Kodama, K and Takayama, H (2003). Intracellular localization of glycoprotein VI in human platelets and its surface expression upon activation. *Br J Haematol* **121**: 904–912.
27. Madoiwa, S, Yamauchi, T, Nakamata, Y, Kobayashi, E, Arai, M, Sugo, T *et al.* (2004). Induction of immune tolerance by neonatal intravenous injection of human factor VIII in murine hemophilia A. *J Thromb Haemost* **2**: 754–762.

THE JOURNAL OF GENE MEDICINE
J Gene Med 2008; **10**: 368–374.
Published online 21 January 2008 in Wiley InterScience (www.interscience.wiley.com) **DOI:** 10.1002/jgm.1166

RESEARCH ARTICLE

Adeno-associated virus vector-mediated systemic interleukin-10 expression ameliorates hypertensive organ damage in Dahl salt-sensitive rats

Mutsuko Nonaka-Sarukawa[1,2]
Takashi Okada[1]
Takayuki Ito[1,2]*
Keiji Yamamoto[2]
Toru Yoshioka[3]
Tatsuya Nomoto[1]
Yukihiro Hojo[2]
Masahisa Shimpo[2]
Masashi Urabe[1]
Hiroaki Mizukami[1]
Akihiro Kume[1]
Uichi Ikeda[3]
Kazuyuki Shimada[2]
Keiya Ozawa[1]*

[1]*Division of Genetic Therapeutics, Jichi Medical University, Japan*

[2]*Division of Cardiovascular Medicine, Jichi Medical University, Japan*

[3]*Department of Organ Regeneration, Shinshu University Graduate School of Medicine, Japan*

*Correspondence to: Takayuki Ito and Keiya Ozawa, Division of Genetic Therapeutics, Centre for Molecular Medicine, Jichi Medical University, 3311-1 Yakushiji, Shimotsuke-shi, Tochigi 329-0498, Japan.
E-mail: titou@jichi.ac.jp and kozawa@jichi.ac.jp

Received: 5 October 2007
Revised: 26 November 2007
Accepted: 11 December 2007

Abstract

Background Inflammation plays an important role in the pathogenesis of hypertension and hypertensive organ damage. Interleukin (IL)-10, a pleiotropic anti-inflammatory cytokine, exerts vasculoprotective effects in many animal models. In the present study, we examined the preventive effects of adeno-associated virus (AAV) vector-mediated sustained IL-10 expression against hypertensive heart disease and renal dysfunction in Dahl salt-sensitive rats.

Methods We injected the rats intramuscularly with an AAV type 1-based vector encoding rat IL-10 or enhanced green fluorescent protein (EGFP) at 5 weeks of age; subsequently, the rats were fed a high-sodium diet from 6 weeks of age.

Results Sustained IL-10 expression significantly improved survival rate of Dahl salt-sensitive rats compared with EGFP expression (62.5% versus 0%, $p < 0.001$); it also caused 26.0% reduction in systolic blood pressure at 15 weeks ($p < 0.0001$). Echocardiography exhibited a 22.0% reduction in hypertrophy ($p < 0.0001$) and a 26.3% improvement in fractional shortening ($p < 0.0001$) of the rat left ventricle in the IL-10 group compared to the EGFP group. IL-10 expression also caused a 21.7% decrease in the heart weight/body weight index and cardiac atrial natriuretic peptide levels. Histopathological studies revealed that IL-10 decreased inflammatory cell infiltration, fibrosis, and transforming growth factor-β_1 levels in the failing heart. Furthermore, IL-10 expression significantly reduced urine protein excretion with increased glomerular filtration rates.

Conclusions This is the first study to demonstrate that the anti-inflammatory cytokine IL-10 has a significant anti-hypertensive effect. AAV vector-mediated IL-10 expression potentially prevents the progression of refractory hypertension and hypertensive organ damage in humans. Copyright © 2008 John Wiley & Sons, Ltd.

Keywords AAV vector; gene therapy; hypertension; inflammation; interleukin-10

Introduction

Inflammation plays an important role in the pathogenesis of hypertension and hypertensive organ damage. Congestive heart failure (CHF) is a crucial life-threatening sequalae of hypertensive organ damage, and

its severity is closely related with the serum tumor necrosis factor (TNF) levels [1,2]. Recent studies have demonstrated the marked anti-hypertensive and renoprotective effects of an immunosuppressant *in vivo* [3,4]. Although these observations suggest a therapeutic potential of anti-inflammatory molecules, anti-TNF antibody treatments (e.g. infliximab and etanercept) have failed to improve the survival of CHF patients partly because of their cytokine-inducing effects and cytotoxicity [5,6].

Interleukin (IL)-10 is a pleiotropic cytokine produced by monocytes/macrophages and type 2 helper T cells. It regulates inflammatory and immune reactions by inhibiting macrophage activation, T-cell proliferation, and the production of proinflammatory cytokines such as TNF-α [7]. IL-10 also enhances endothelial nitric oxide synthase expression [8] and inhibits vascular smooth muscle cell proliferation [9,10]. Previous studies have demonstrated the therapeutic effects of IL-10 on CHF models resulting from acute viral or autoimmune myocarditis [11,12]. However, no studies have examined the effects of IL-10 on chronic CHF resulting from hypertensive heart disease that occurs far more frequently than acute myocarditis. In the present study, we examined the effects of IL-10 using Dahl salt-sensitive (DS) rats that present with severe hypertension and chronic CHF when fed a salt-rich diet [13].

We employed an adeno-associated virus (AAV) type 1-based vector in order to sustain serum levels of IL-10 because it has a short biological half-life. AAV vectors permit long-term transgene expression with minimal inflammatory and immune responses [14]. If the intramuscular injection of the AAV serotype 1 vector carrying the IL-10 gene (AAV1-IL-10) produces sufficient amount of IL-10 in skeletal myocytes, then IL-10 should be secreted into the systemic circulation [10]. We examined the preventive effects of IL-10 on chronic CHF progression in DS rats, focusing on its effects on survival, hypertension, pathological cardiac remodelling and renal function.

Materials and methods

AAV vector production

Rat IL-10 was cloned from rat splenocyte cDNA by the polymerase chain reaction (PCR) using the primers: 5′-GCACGAGAGCCACAACGCA-3′ (upstream) and 5′-GATTTGAGTACGATCCATTTATTCAAAACGAGGAT-3′ (downstream) [10]. To achieve efficient transduction of the skeletal muscles, we developed a recombinant AAV type 1-based vector encoding rat IL-10 (AAV1-IL-10) or enhanced green fluorescence protein (EGFP, AAV1-EGFP) controlled by the modified chicken β-actin promoter with the cytomegalovirus immediate–early enhancer and by the woodchuck hepatitis virus post-transcriptional regulatory element [pBS II SK (+) WPRE-B11, provided by Dr Thomas Hope, University of Illinois, Chicago, IL, USA]. The AAV vectors were prepared by the previously described three-plasmid transfection adenovirus-free protocol modified by the use of the active gassing system [15,16]. Briefly, 60% confluent human embryonic kidney 293 cells were co-transfected with the proviral transgene plasmid, the AAV-1 chimeric helper plasmid p1RepCap (provided by Dr James M. Wilson, University of Pennsylvania, Philadelphia, PA, USA), and the adenoviral helper plasmid pAdeno (provided by Avigen, Inc., Alamada, CA, USA). The crude viral lysate was purified by two rounds of two-tier CsCl centrifugation [14]. The viral stock titer was determined by dot blot hybridization with plasmid standards.

Animal experiment protocols

All animal studies were performed in accordance with the guidelines issued by the committee on animal research and approved by the ethics committee of Jichi Medical University. For histopathological and physiological studies (Protocol 1; Figure 1), we divided the male DS rats (Japan SLC, Shizuoka, Japan) into the following three groups:

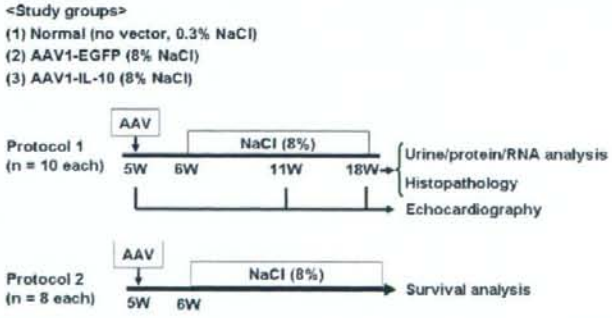

Figure 1. Study protocols. The male DS rats were divided into the three groups: (1) normal group, (2) EGFP group, and (3) IL-10 group. The rats without normal group were injected with AAV1 vectors at 5 weeks of age. The rats in the normal group were fed a low-sodium diet (containing 0.3% NaCl), whereas those in the EGFP or IL-10 group were fed a high-sodium diet (containing 8% NaCl) from 6 weeks of age

DOI: 10.1002/jgm

IL-10, EGFP and normal ($n = 10$, respectively). AAV1-IL-10 or AAV1-EGFP [1×10^{12} genome copies (g.c.)/body] was injected bilaterally into the anterior tibial muscles of the 5-week-old rats in the IL-10 or EGFP groups, respectively. From 6 weeks onwards, these rats were fed a high-sodium diet (containing 8% NaCl). DS rats in the normal group were fed a low-sodium diet (containing 0.3% NaCl). Systolic blood pressure (SBP) was measured every 2 weeks by the tail-cuff method using a manometer tachometer (MK-1030; Muromachi Kikai Co., Ltd, Tokyo, Japan). During the acclimatization period (3–5 weeks), training for blood pressure measurements was performed three times a week. The mean of the three measurements following a 10-min rest at 37 °C was used in the calculations. Blood was collected from the tail vein at 5,11 and 18 weeks; the sera and plasma were stored at −80 °C. At 18 weeks, the rats were sacrificed by administering an overdose of isoflurane, and their hearts and lungs were harvested and weighed. The tissues were immediately frozen in liquid nitrogen and stored at −80 °C to obtain proteins and RNA for the subsequent analysis. For survival analysis (Protocol 2; Figure 1), the rats were randomly divided into three groups ($n = 8$ each). Those in the IL-10 or EGFP group were injected at 5 weeks of age with the AAV1-IL-10 or AAV1-EGFP (1×10^{11} g.c./body), respectively, and this was followed by a high-sodium diet from 6 weeks of age. By contrast, those in the normal group were fed a low-sodium diet.

Echocardiography

Transthoracic two-dimensional echocardiography was performed at 5, 11 and 18 weeks of age using a 13- MHz transducer (ProSound SSD-α5; Aloka Co., Ltd, Tokyo, Japan). The internal diameter in end-diastole or end-systole of the left ventricle (LVDd or LVDs, respectively) or the posterior wall thickness (PWT) of the left ventricle (LV) in end-diastole was measured by M-mode tracing at the papillary muscle level. The relative wall thickness (RWT) or the percentage fractional shortening (%FS) of LV was calculated according to the formula: RWT = $2 \times$ PWT/LVDd, %FS = (LVDd − LVDs)/LVDd $\times$ 100 (%).

Cytokine measurements

At 18 weeks, protein samples were prepared by homogenizing the frozen heart tissues in a lysis buffer [10 mmol/l Tris-HCl (pH 8.0), 0.2% NP40, 1 mmol/l ethylenediaminetetraacetic acid] containing the protease inhibitor cocktail Complete Mini (Roche Diagnostics, Mannheim, Germany). After centrifugation of the homogenates or serum samples, the supernatants were used for measurement. The serum IL-10 and the tissue transforming growth factor (TGF)-β_1 concentrations were measured by enzyme-linked immunosorbent assay (ELISA) (Amersham PharmaciaBiotech, Bucks, UK; BioSource International, Inc., Camarillo, CA, USA; R&D Systems Inc., Minneapolis, MN, USA). The tissue cytokine levels were standardized using the total protein concentrations estimated by the BCA Protein Assay Kit (Pierce, Rockford, IL, USA).

Quantitative reverse transcriptase (RT)-PCR

At 18 weeks, total RNA was extracted from the heart by using RNAzol B (Tel-Test, Inc., Friendswood, TX, USA) and reverse-transcribed into double-stranded cDNA by using the Superscript Preamplification System (Invitrogen, Carlsbad, CA, USA) with the T7-dT primer (5′-GGCCAGTGAATTGTAATACGACTCACTATAGGGA-GGCGGTTTTTTTTTTTTTTTTTTTTTTTT-3′). To estimate the atrial natriuretic protein (ANP) mRNA levels, quantitative PCR analysis was conducted using the ABI Prism 7900 Sequence Detection System (Applied Biosystems, Foster City, CA, USA). The GAPDH mRNA was quantified for normalization. The oligonucleotide primers used were: for GADPH, 5′-CAGCAATGCAT CCTGCAC-3′ (upstream) and 5′-GAGTTGCTGTTGAAGTCACAGG-3′ (downstream) [17]; for ANP, 5′-GGTAGGATTGACAGGATTGGAGCC-3′ (upstream) and 5′-ACATCGATCGTGATAGATGAAGAC-3′ (downstream) [18]. Quantitative values were obtained from the threshold cycle (C_t) number that indicates exponential amplification of a PCR product.

Histopathology

At 18 weeks of age, the anesthetized rats were perfused with 50 ml of saline, followed by 100 ml of cold 4% paraformaldehyde in 0.1 mol/l phosphate buffer (pH 7.4). The hearts were fixed in the same fixative and finally embedded in paraffin. For evaluation of light microscopic findings, we stained sections (3 µm thick) with hematoxylin and eosin (H&E) or the Azan–Mallory stain using the standard methods.

Statistical analysis

The data were assessed using the StatView, version 5.0 (Statview, Abacus Concepts, Berkeley, CA, USA). Differences in the values at specific stages between the groups were assessed by one-way analysis of variance combined with Fisher's test. $p < 0.05$ was considered statistically significant. Survival curves were analysed by the Kaplan–Meier method and compared using log-rank tests.

Results

Pro-survival effect of systemic IL-10 in DS rats

Compared to the control EGFP transduction, IL-10 transduction significantly improved survival rates in DS

rats fed a high-sodium diet ($p < 0.001$, Figure 2). After 13 weeks of the gene delivery, serum IL-10 concentrations significantly increased in the IL-10-transduced rats compared to the normal untreated rats or control EGFP-transduced rats (986.6 ± 278.5 pg/ml versus <3 or 20.8 ± 18.1 pg/ml, $p < 0.001$, respectively; Figure 3). At this time point, the EGFP transduction generated a slight but significant increase of endogenous IL-10 levels compared to control ($p < 0.01$).

Anti-hypertensive effects of IL-10

SBP gradually increased in the EGFP group, resulting in levels of 184 ± 7 mmHg at 15 weeks of age (Figure 4). At 9 weeks (i.e. after 4 weeks of the vector injection), SBP in the IL-10 group (151 ± 7 mmHg) was significantly lower

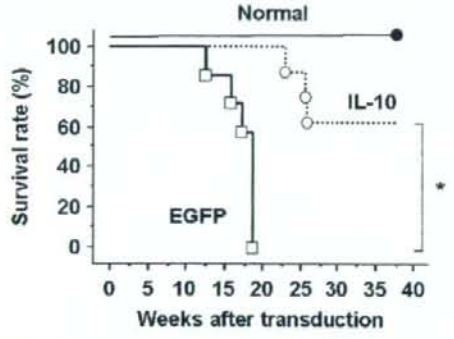

Figure 2. The pro-survival effects of IL-10 in DS rats. The 5-week-old rats were intramuscularly injected with AAV1-IL-10 or AAV1-EGFP at 1×10^{11} g.c./body. Kaplan–Meier survival analysis was performed. Closed circle, normal group; open circles, IL-10 group; open squares, EGFP group ($n = 8$ each). $^{*}p < 0.001$ versus EGFP group

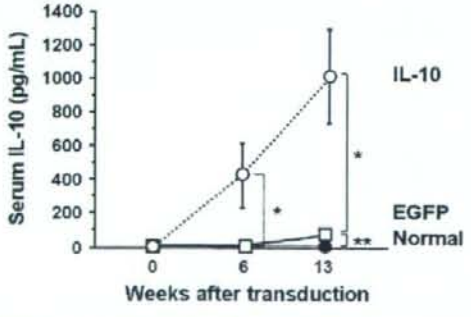

Figure 3. AAV vector-mediated systemic IL-10 expression in DS rats. AAV1-EGFP or AAV1-IL-10, at 1×10^{12} g.c./body, respectively, was injected bilaterally into the anterior tibial muscles of the 5-week-old rats. Serum IL-10 levels were determined periodically by ELISA. The normal group includes DS rats fed a low-sodium diet and not administered the vector injection. The results are presented as means ± SD ($n = 10$ each). $^{*}p < 0.001$, $^{**}p < 0.01$

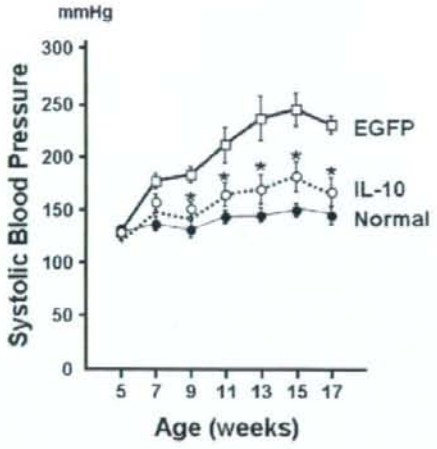

Figure 4. The anti-hypertensive effect of IL-10. Longitudinal tracing of systolic blood pressure evaluated by the tail-cuff method after injecting the AAV vectors in 5-week-old DS rats. Open squares, EGFP group; open circles, IL-10 group; closed circles, normal group ($n = 10$ each). The results are presented as means ± SD. $^{*}p < 0.001$ versus EGFP group

Table 1. Effects of IL-10 on left ventricular hypertrophy and function

	RWT (mm)		%FS (%)	
Age (weeks)	5	11	5	18
Normal	0.46 ± 0.03	0.48 ± 0.02	58.7 ± 3.7	57.2 ± 3.9
EGFP	0.45 ± 0.03	0.63 ± 0.04*	59.8 ± 1.9	32.9 ± 4.4*
IL-10	0.45 ± 0.04	0.49 ± 0.02**	59.4 ± 2.6	59.2 ± 4.6**

M-mode echocardiograms of the LV at the papillary muscle level were traced for analysis. RWT of the LV as an index of LV hypertrophy and %FS as an index of systolic LV function were calculated as described in the Materials and methods. The results are presented as means ± SD ($n = 10$ each). $^{*}p < 0.0001$ versus Normal group, $^{**}p < 0.0001$ versus EGFP group at the same time-point, respectively.

than that in the EGFP group ($p < 0.0001$). The anti-hypertensive effect of IL-10 persisted until the animals were sacrificed at 18 weeks of age.

Effects of IL-10 on left ventricular hypertrophy, function and CHF

Echocardiography exhibited a 22.0% reduction in the RWT of the LV posterior wall at 11 weeks of age ($p < 0.0001$) and a 26.3% improvement in %FS of the LV wall at 18 weeks of age ($p < 0.0001$) in the IL-10 group compared to the EGFP group (Table 1). As compared to EGFP expression, IL-10 expression caused a 21.7% or 52.7% decrease in the heart or lung weight/body weight index, respectively (all $p < 0.05$; Figures 5a and 5b). Similarly, the cardiac ANP mRNA level significantly increased in the EGFP group compared to the control (46.5 ± 23.8-fold); whereas, IL-10 transduction significantly suppressed this increase (9.28 ± 5.2-fold) compared to control (Figure 5c).

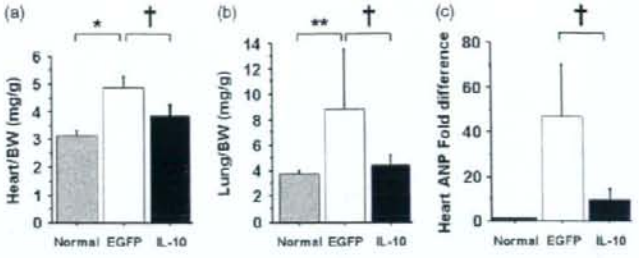

Figure 5. Effects of IL-10 on congestive heart failure. The hearts (a) and lungs (b) of DS rats were harvested and weighed at 18 weeks of age. Data were expressed after normalization using body weight. The cardiac ANP mRNA levels determined by real-time RT-PCR (c). The total RNA was extracted from the heart at 18 weeks of age. The mRNA levels were corrected by using the GAPDH mRNA level of each animal and then normalized to the mean value of the normal group. The results are presented as means ± SD ($n = 10$ each). $^{*}p < 0.01$ versus Normal group, $^{**}p < 0.05$ versus Normal group, $\dagger p < 0.05$ versus EGFP

Effects of IL-10 on pathological cardiac remodelling

H&E staining demonstrated increased interstitial and perivascular cell infiltration in the failing heart of the EGFP-transduced rats (Figure 6a). Azan–Mallory staining demonstrated that interstitial and perivascular fibrosis increased in the EGFP group (Figure 6b). IL-10 transduction inhibited fibrosis and significantly decreased the cardiac TGF-β_1 levels in DS rats compared to the EGFP transduction (64.5 ± 45.3 pg/mg protein versus 197.1 ± 91.9 pg/mg protein, $p < 0.05$; Figure 6c).

Effects of IL-10 on renal function

Compared to control rats, DS rats fed a high-sodium diet exhibited a 68.0% increase in serum creatinine, a 243.0% increase in urine protein levels, and a 49.9% decrease in glomerular filtration rate (all $p < 0.05$; Figure 7). Sustained IL-10 expression reduced these changes by 88.2%, 100% and 45.8%, respectively (all $p < 0.05$).

Discussion

The present study demonstrates that systemic IL-10 expression via the AAV serotype 1 vector prevented the progression of hypertension, CHF and renal dysfunction in DS rats. A single intramuscular injection of AAV1-IL-10 achieved long-term systemic IL-10 expression, leading to the prolonged survival of the rats. The IL-10 transduction not only preserved systolic LV function, but also reduced fibrosis of the LV at the heart failure phase. The anti-hypertensive effect of IL-10 occurred prior to the

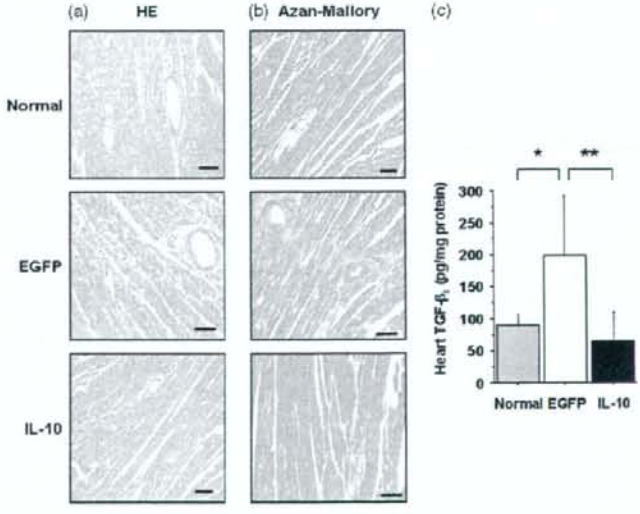

Figure 6. Histopathology and cardiac TGF-β_1 levels of the 18-week-old DS rats. (a) Representative micrographs of the H&E staining. (b) Representative micrographs of Azan–Mallory staining. Magnification, ×200; scale bar = 100 μm. (c) TGF-β_1 concentrations in the heart homogenates determined by ELISA. The results are presented as means ± SD ($n = 10$ each). $^{*}p < 0.05$ versus Normal group, $^{**}p < 0.05$ versus EGFP group

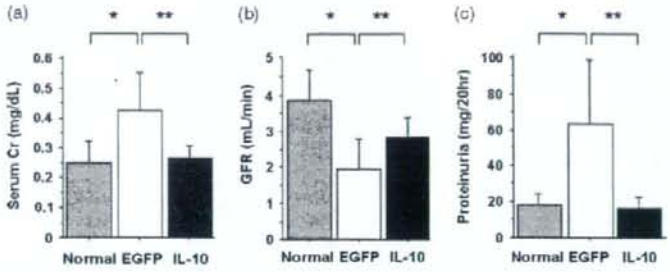

Figure 7. Effects of IL-10 on renal function in DS rats. (a) Serum creatinine (Cr), (b) glomerular filtration rate (GFR) and (c) urine protein levels were determined at 18 weeks of age. The results are presented as means ± SD ($n = 10$ each). *$p < 0.001$ versus Normal group, **$p < 0.05$ versus EGFP group

development of CHF and LVH, suggesting that this effect may largely contribute to amelioration of sodium-induced hypertensive organ damage.

Many studies have suggested the therapeutic potentials of IL-10 for CHF. Serum IL-10 levels decrease in CHF patients [19], and exogenous IL-10 administration retards progression of the disease in many cardiovascular disease models [20]. However, these studies used CHF models in which CHF was a result of acute viral or autoimmune myocarditis, and they examined the short-term IL-10 effects against initial inflammatory responses [11,12]. In the present study, we demonstrated the effects of long-term IL-10 expression against chronic CHF progression, hypertension and inflammatory changes of the cardiac tissue.

We detected a slight but significant increase of endogenous IL-10 levels in the heart failure phase in control DS rats. However, this increase was insufficient to cause beneficial effects. On the other hand, conventional IL-10 therapies based on recombinant drugs or plasmids require frequent administration for sufficient and sustained IL-10 expression. Thus, we used AAV vectors that permit long-term transgene expression *in vivo* [14]. Previously, we demonstrated that a single intramuscular injection of the AAV5-based vector caused systemic IL-10 expression for 1 year [21]. Since AAV1 is more efficient for muscle transduction than AAV2 or AAV5 [22], we used AAV1 as the vector in the present study [23].

A clinical trial using infliximab, a chimeric monoclonal antibody to TNF-α, failed to prolong the survival of CHF patients over the long term [5]. We speculate that the failure might be in part based on an insufficient regulation of the cytokine network, which may be involved in the progression of CHF and other related diseases such as hypertension and renal failure. Recent studies have shown the marked anti-hypertensive effects of an immunosuppressant mycophenolate mofetil (MMF) in DS rats [3,4]. MMF administration also ameliorates renal dysfunction via anti-inflammatory effects. Interestingly, an intramuscular injection of AAV1-IL-10 successfully ameliorated renal function in a rat model after nephrectomy [24]. We also observed that systemic IL-10 expression significantly attenuated hypertension and renal dysfunction, along with a decrease of inflammatory cell infiltration, in the kidney of stroke-prone spontaneously hypertensive rats (T. Nomoto *et al.*, unpublished data). In the present study, we demonstrate that IL-10 gene therapy successfully ameliorated heart failure and renal dysfunction along with a suppression of severe hypertension in DS rats. These observations suggest that anti-inflammatory action of IL-10 may attenuate the target organ damage related to high blood pressure. However, precise mechanism underlying the anti-hypertensive effect of IL-10 require further investigation.

The synthesis of ANP, a cardioprotective hormone predominantly produced by the ventricle, as well as its circulating levels, increases in accordance with the severity of CHF [25,26]. Administration of exogenous ANP ameliorates CHF in clinical settings via its diuretic and vasodilatory effects. In the present study, the cardiac ANP mRNA level significantly decreased in the IL-10 group. These observations suggest that IL-10 ameliorated CHF independently of direct ANP production but inhibited the adaptive increase in ANP levels.

The present study demonstrates that IL-10 expression attenuated pathological cardiac remodelling with reduced expression of TGF-β_1, a hallmark of cardiac fibrosis in DS rats [27]. Expression of monocyte chemoattractant protein (MCP)-1 in the endothelium of intramyocardial arterioles triggers perivascular macrophage accumulation [28]. Macrophage infiltration induces TGF-β_1 production, leading to fibroblast proliferation and extracellular matrix production [29]. Interestingly, a neutralizing antibody against TGF-β inhibits fibroblast activation, resulting in reduced collagen production and subsequent myocardial fibrosis [30]. Previously, we reported that systemic IL-10 expression significantly decreased serum MCP-1 levels, perivascular macrophage infiltration, and pulmonary tissue TGF-β_1 levels *in vivo* [10,21]. These observations suggest that the reduced macrophage-derived TGF-β_1 expression following MCP-1 suppression might be responsible for the anti-remodelling effects of IL-10. However, the direct effects of IL-10 on TGF-β_1 in the pathogenesis of CHF remain unclear.

Epidemiological studies have demonstrated that the increased pro-inflammatory cytokine expression is related to the incidence of pre-hypertension [31]. These results

suggest a possible link between the inflammatory response and the development of hypertension. This is the first study to demonstrate the anti-hypertensive effects of IL-10, which might be a key molecule to explain this relationship. Exploring the mechanisms underlying the effects of IL-10 would provide new molecular targets for refractory hypertension and its sequalae.

In conclusion, the sustained IL-10 expression achieved by the single AAV-IL-10 injection ameliorated CHF and prolonged survival in DS rats. IL-10 expression attenuated salt-sensitive hypertension, LV remodelling and renal dysfunction. These results suggest that our IL-10-based strategy potentially prevents the progression of refractory hypertensive organ damage in humans.

Acknowledgements

We thank Miyoko Mitsu and Takako Takagi for their encouragement and technical support. This work was supported by grants from the Ministry of Health, Labour and Welfare of Japan. This work was also supported by Grants-in-Aid for Scientific Research; a grant from the 21 Century COE program; and High-Tech Research Centre Project for Private Universities, matching fund subsidy, from the Ministry of Education, Culture, Sports, Science and Technology of Japan; and a research award to Jichi Medical School Graduate Student. This work was performed at Jichi Medical University in Shimotuke-shi, Tochigi, Japan.

References

1. Levine B, Kalman J, Mayer L, *et al.* Elevated circulating levels of tumor necrosis factor in severe chronic heart failure. *N Engl J Med* 1990; **323**: 236–241.
2. Vasan RS, Sullivan LM, Roubenoff R, *et al.* Inflammatory markers and risk of heart failure in elderly subjects without prior myocardial infarction: the Framingham Heart Study. *Circulation* 2003; **107**: 1486–1491.
3. Mattson DL, James L, Berdan EA, *et al.* Immune suppression attenuates hypertension and renal disease in the Dahl salt-sensitive rat. *Hypertension* 2006; **48**: 149–156.
4. Tian N, Gu JW, Jordan S, *et al.* Immune suppression prevents renal damage and dysfunction and reduces arterial pressure in salt-sensitive hypertension. *Am J Physiol Heart Circ Physiol* 2007; **292**: H1018–H1025.
5. Chung ES, Packer M, Lo KH, *et al.* Randomized, double-blind, placebo-controlled, pilot trial of infliximab, a chimeric monoclonal antibody to tumor necrosis factor-alpha, in patients with moderate-to-severe heart failure: results of the anti-TNF Therapy Against Congestive Heart Failure (ATTACH) trial. *Circulation* 2003; **107**: 3133–3140.
6. Mann DL, McMurray JJ, Packer M, *et al.* Targeted anticytokine therapy in patients with chronic heart failure: results of the Randomized Etanercept Worldwide Evaluation (RENEWAL). *Circulation* 2004; **109**: 1594–1602.
7. Elenkov IJ, Chrousos GP. Stress hormones, proinflammatory and antiinflammatory cytokines, and autoimmunity. *Ann NY Acad Sci* 2002; **966**: 290–303.
8. Cattaruzza M, Slodowski W, Stojakovic M, *et al.* Interleukin-10 induction of nitric-oxide synthase expression attenuates CD40-mediated interleukin-12 synthesis in human endothelial cells. *J Biol Chem* 2003; **278**: 37874–37880.
9. Selzman CH, McIntyre RC, Jr., Shames BD, *et al.* Interleukin-10 inhibits human vascular smooth muscle proliferation. *J Mol Cell Cardiol* 1998; **30**: 889–896.
10. Ito T, Okada T, Miyashita H, *et al.* Interleukin-10 expression mediated by an adeno-associated virus vector prevents monocrotaline-induced pulmonary arterial hypertension in rats. *Circ Res* 2007; **101**: 734–741.
11. Nishio R, Matsumori A, Shioi T, *et al.* Treatment of experimental viral myocarditis with interleukin-10. *Circulation* 1999; **100**: 1102–1108.
12. Palaniyandi SS, Watanabe K, Ma M, *et al.* Inhibition of mast cells by interleukin-10 gene transfer contributes to protection against acute myocarditis in rats. *Eur J Immunol* 2004; **34**: 3508–3515.
13. Kihara Y, Sasayama S. Transition from compensatory hypertrophy to dilated failing left ventricle in Dahl-Iwai salt-sensitive rats. *Am J Hypertens* 1997; **10**: 78S–82S.
14. Okada T, Shimazaki K, Nomoto T, *et al.* Adeno-associated viral vector-mediated gene therapy of ischemia-induced neuronal death. *Methods Enzymol* 2002; **346**: 378–393.
15. Matsushita T, Elliger S, Elliger C, *et al.* Adeno-associated virus vectors can be efficiently produced without helper virus. *Gene Ther* 1998; **5**: 938–945.
16. Okada T, Nomoto T, Yoshioka T, *et al.* Large-scale production of recombinant viruses by use of a large culture vessel with active gassing. *Hum Gene Ther* 2005; **16**: 1212–1218.
17. Nakahara T, Hashimoto K, Hirano M, *et al.* Acute and chronic effects of alcohol exposure on skeletal muscle c-myc, p53, and Bcl-2 mRNA expression. *Am J Physiol Endocrinol Metab* 2003; **285**: E1273–1281.
18. Ueno S, Ohki R, Hashimoto T, *et al.* DNA microarray analysis of in vivo progression mechanism of heart failure. *Biochem Biophys Res Commun* 2003; **307**: 771–777.
19. Stumpf C, Lehner C, Yilmaz A, *et al.* Decrease of serum levels of the anti-inflammatory cytokine interleukin-10 in patients with advanced chronic heart failure. *Clin Sci (Lond)* 2003; **105**: 45–50.
20. Ito T, Ikeda U. Inflammatory cytokines and cardiovascular disease. *Curr Drug Targets Inflamm Allergy* 2003; **2**: 257–265.
21. Yoshioka T, Okada T, Maeda Y, *et al.* Adeno-associated virus vector-mediated interleukin-10 gene transfer inhibits atherosclerosis in apolipoprotein E-deficient mice. *Gene Ther* 2004; **11**: 1772–1779.
22. Hauck B, Chen L, Xiao W. Generation and characterization of chimeric recombinant AAV vectors. *Mol Ther* 2003; **7**: 419–425.
23. Ito T, Okada T, Mimuro J, *et al.* Adenoassociated virus-mediated prostacyclin synthase expression prevents pulmonary arterial hypertension in rats. *Hypertension* 2007; **50**: 531–536.
24. Mu W, Ouyang X, Agarwal A, *et al.* IL-10 suppresses chemokines, inflammation, and fibrosis in a model of chronic renal disease. *J Am Soc Nephrol* 2005; **16**: 3651–3660.
25. Saito Y, Nakao K, Arai H, *et al.* Augmented expression of atrial natriuretic polypeptide gene in ventricle of human failing heart. *J Clin Invest* 1989; **83**: 298–305.
26. de Boer RA, Henning RH, Suurmeijer AJ, *et al.* Early expression of natriuretic peptides and SERCA in mild heart failure: association with severity of the disease. *Int J Cardiol* 2001; **78**: 5–12.
27. Ichihara S, Obata K, Yamada Y, *et al.* Attenuation of cardiac dysfunction by a PPAR-alpha agonist is associated with down-regulation of redox-regulated transcription factors. *J Mol Cell Cardiol* 2006; **41**: 318–329.
28. Kuwahara F, Kai H, Tokuda K, *et al.* Hypertensive myocardial fibrosis and diastolic dysfunction: another model of inflammation? *Hypertension* 2004; **43**: 739–745.
29. Border WA, Noble NA. Transforming growth factor beta in tissue fibrosis. *N Engl J Med* 1994; **331**: 1286–1292.
30. Kuwahara F, Kai H, Tokuda K, *et al.* Transforming growth factor-beta function blocking prevents myocardial fibrosis and diastolic dysfunction, in pressure-overloaded rats. *Circulation* 2002; **106**: 130–135.
31. Chrysohoou C, Pitsavos C, Panagiotakos DB, *et al.* Association between prehypertension status and inflammatory markers related to atherosclerotic disease: the ATTICA Study. *Am J Hypertens* 2004; **17**: 568–573.

Protection Against Aminoglycoside-induced Ototoxicity by Regulated AAV Vector–mediated GDNF Gene Transfer Into the Cochlea

Yuhe Liu[1,2,3], Takashi Okada[1,4], Kuniko Shimazaki[5], Kianoush Sheykholeslami[6], Tatsuya Nomoto[1], Shin-Ichi Muramatsu[7], Hiroaki Mizukami[1], Akihiro Kume[1], Shuifang Xiao[3], Keiichi Ichimura[2] and Keiya Ozawa[1]

[1]*Division of Genetic Therapeutics, Jichi Medical University, Tochigi, Japan;* [2]*Department of Otolaryngology, Jichi Medical University, Tochigi, Japan;* [3]*Department of Otolaryngology, Peking University First Hospital, Beijing, China;* [4]*Department of Molecular Therapy, National Institute of Neuroscience, National Center of Neurology and Psychiatry, Tokyo, Japan;* [5]*Department of Physiology, Jichi Medical University, Tochigi, Japan;* [6]*Department of Neurobiology, Northeastern Ohio Universities College of Medicine, Rootstown, Ohio, USA;* [7]*Division of Neurology, Department of Medicine, Jichi Medical University, Tochigi, Japan*

Since standard aminoglycoside treatment progressively causes hearing disturbance with hair cell degeneration, systemic use of the drugs is limited. Adeno-associated virus (AAV)-based vectors have been of great interest because they mediate stable transgene expression in a variety of postmitotic cells with minimal toxicity. In this study, we investigated the effects of regulated AAV1-mediated glial cell line–derived neurotrophic factor (GDNF) expression in the cochlea on aminoglycoside-induced damage. AAV1-based vectors encoding GDNF or vectors encoding GDNF with an rtTA2s-S2 Tet-on regulation system were directly microinjected into the rat cochleae through the round window at 5×10^{10} genome copies/body. Seven days after the virus injection, a dose of 333 mg/kg of kanamycin was subcutaneously given twice daily for 12 consecutive days. GDNF expression in the cochlea was confirmed and successfully modulated by the Tet-on system. Monitoring of the auditory brain stem response revealed an improvement of cochlear function after GDNF transduction over the frequencies tested. Damaged spiral ganglion cells and hair cells were significantly reduced by GDNF expression. Our results suggest that AAV1-mediated expression of GDNF using a regulated expression system in the cochlea is a promising strategy to protect the cochlea from aminoglycoside-induced damage.

Received 12 May 2007; accepted 15 November 2007; published online 8 January 2008. doi:10.1038/sj.mt.6300379

INTRODUCTION

Aminoglycoside antibiotics are frequently used in empiric therapy for serious infections, such as septicemia, complicated intra-abdominal infections, complicated urinary tract infections, and nosocomial respiratory tract infections. However, it is well known that aminoglycosides are associated with severe side effects, such as ototoxicity and nephrotoxicity, which attack the cochlea or vestibule and destroys the auditory and vestibular hair cells that pass information to the auditory nerve.[1] In addition, aminoglycosides predominantly destroy the outer hair cells by ototoxicity. Although the exact mechanism of damage is not well established,[2] aminoglycoside-induced hair cell loss results in a permanent hearing deficit[3] that can progressively occur 6 months to a year after exposure to these drugs. Therefore, the development of a strategy to prevent aminoglycoside-associated ototoxicity before adverse events occur is a critical issue in clinical settings.

The expression of a transgene using viral vectors is a potential approach to introduce neurotrophic factors into the cochlea to prevent and treat aminoglycoside-induced hearing loss. However, most of the currently used vectors, such as adenovirus vectors or herpes simplex virus vectors, have an associated vector-related cytotoxicity.[4,5] Hence, adeno-associated virus (AAV) vectors may be good candidates for gene transfer into the cochlear cells because of their efficient transduction and their safety and potential in long-term expression.[6] We have previously demonstrated that an AAV1-based vector efficiently transduced the inner hair cells, the spiral ganglion cells, and many other types of cells.[7] Therefore, an AAV1-based vector should successfully introduce secretory proteins, such as glial cell line–derived neurotrophic factor (GDNF), into the cochlea to prevent aminoglycoside-induced ototoxicity.

GDNF, a member of the transforming growth factor β family, was initially identified as a survival factor for mid-brain dopaminergic neurons and for a wide range of neuronal populations in the central and peripheral nervous systems.[8–10] Although it is still unclear whether GDNF protects against ototoxicity, sustained infusion of recombinant GDNF protected the cochlear structure and function from noise- and drug-induced damage and stress,[11–16] although its half-life is very short. However, an overdose of GDNF was shown to enhance the sensitivity of the cochleae to insult and

Correspondence: *Takashi Okada, Department of Molecular Therapy, National Institute of Neuroscience, National Center of Neurology and Psychiatry, 4-1-1 Ogawa-Higashi, Kodaira, Tokyo 187-8551, Japan. E-mail: t-okada@ncnp.go.jp; Keiya Ozawa, Division of Genetic Therapeutics, Center for Molecular Medicine, Jichi Medical University, 3311-1 Yakushiji, Shimotsuke, Tochigi 329-0498, Japan. E-mail: kozawo@jichi.ac.jp*

to destroy cochlear function.[12] Furthermore, it has been reported that testicular tumors are formed in GDNF-overexpressing mice.[19] Therefore, an appropriate regulation system is required to realize the therapeutic benefits of GDNF expression.

Regulated transgene expression has been successfully achieved in various gene therapy experiments using the Tet system.[20–23] Notably, tetracycline derivatives, such as doxycycline (Dox), activate the Tet-on system at doses 100-fold lower than tetracycline. Furthermore, the reverse Tet-responsive transcriptional activator (rtTA) series were improved through the generation of variants called rtTA2s-S2, which showed lower leakiness and better inducibility in HeLa cells and mice.[24,25]

In this study, we describe *in vivo* therapeutic experiments utilizing AAV1 vector–mediated tetracycline-regulated expression of GDNF in cochleae. We demonstrate that AAV1 vector–mediated GDNF expression protects sensory cells in the inner ear from drug-induced degeneration.

RESULTS

Expression and distribution of transgene in the cochlea

AAV1-EGFP or AAV1-GDNF containing either the enhanced humanized green fluorescent protein (*EGFP*) gene or the *GDNF* gene under the control of the CAG (human cytomegalovirus (CMV) immediate-early enhancer and Chicken β-actin promoter) promoter, and the Woodchuck hepatitis virus posttranscriptional regulatory element (WPRE) (Figure 1a), was injected into the cochlea. The GDNF protein level in the perilymph was measured by enzyme-linked immunosorbent assay (Figure 2a). There was a significant increase in GDNF concentration in the cochlea transduced with AAV1-GDNF. The widespread distribution of the GDNF expression was observed in the cochlea, including the spiral ganglion and the inner hair cells (Figure 2b).

To examine the possible transduction of the contralateral ear with the virus diffusion, we analyzed the AAV vector–meditated transgene expression of the rodents with this transduction approach using the optical bioluminescence imaging. Luciferase expression was mainly detected at the injected side of the cochleae (5,370.3 photons/sec/cm^2/sr, **Supplementary Figure S1**). Interestingly, the AAV vector also transduced the contralateral ear (876.8 photons/sec/cm^2/sr), along with the brain (792.9 photons/sec/cm^2/sr). Similar results were obtained with repeated experiments.

Preservation of the hair cells and spiral ganglion cells in the cochlea

Hair cell loss in the whole-mount cochleae of all the tested rat groups was analyzed by F-actin staining with rhodamine–phalloidin. Figure 3a shows a representative dissection through the second turn of the rat cochlea, in which a full complement of hair cells is revealed by F-actin phalloidin staining. In the vehicle-treated control group, outer hair cells in the base and middle turn were drastically lost after kanamycin treatment (Figure 3b). In the AAV1-GDNF/kanamycin-treated group, successful protection of the hair cells in the cochlea was observed (Figure 3c). In the contralateral cochlea, some of outer hair cells were also protected (Figure 3d). The spiral ganglion cell loss in the basal turn of the cochlea was assessed using 4′,6-diamino-2-phenylindole dihydrochloride staining (Figure 4a and b). Survival of the spiral ganglion cells in the AAV1-GDNF injected cochlea was significantly improved compared to that in the AAV1-EGFP injected cochlea (Figure 4c).

Protection of cochlear function by GDNF

Auditory brain stem response (ABR) recordings of the aminoglycoside-treated animals were performed to examine hearing

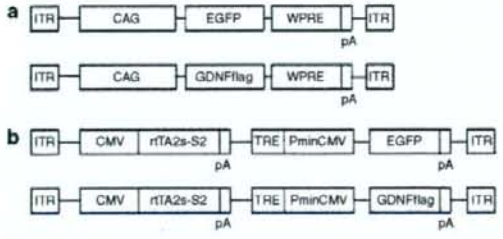

Figure 1 Schematic representation of the viral vectors used in this study. (**a**) An adeno-associated virus 1 (AAV1)-based vector was constructed using the CAG promoter to drive enhanced green fluorescent protein (EGFP) or mouse glial cell line–derived neurotrophic factor (GDNF) with a FLAG tag (GDNFflag). The Woodchuck hepatitis virus posttranscriptional regulatory element (WPRE) was inserted into the 3′ end of the transgene cassette. (**b**) The transactivator rtTA2s-S2 is under the control of the CMV promoter. The minimal CMV promoter (PminCMV) induces transgene expression (EGFP or GDNFflag) in combination with the Tetracycline-responsive element (TRE) and transactivator. CAG, human cytomegalovirus immediate-early enhancer and Chicken β-actin promoter; CMV, cytomegalovirus immediate-early promoter; pA, the simian virus 40 polyadenylation sequences; ITR, inverted terminal repeat from AAV2.

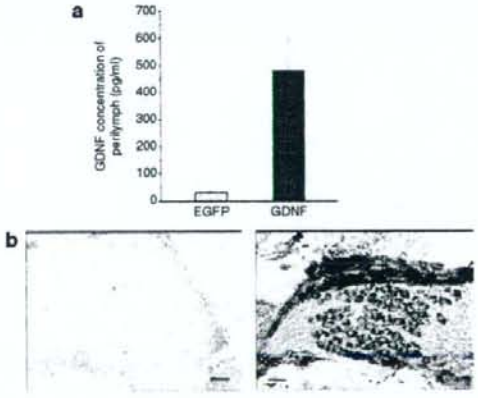

Figure 2 Expression and distribution of transgene in the cochlea. (**a**) Cochlear glial cell line–derived neurotrophic factor (GDNF) expression levels were measured by enzyme-linked immunosorbent assay in the transduced rats. GDNF expression level of the perilymph in the AAV1-GDNF/kanamycin group was significantly higher than that in the control group ($n = 5$, $P < 0.001$). (**b**) Immunohistochemistry was performed to analyze the expression of the GDNFflag in the rat cochlea. The AAV1-EGFP-transduced cochlea was used as a control (left). Cochlear sections were prepared after AAV1-GDNF injection and kanamycin administration. GDNFlag expression was detected in the cochlea with an anti-FLAG antibody (right). Scale bar = 25 µm; ×400. AAV1, adeno-associated virus 1; EGFP, enhanced green fluorescent protein.

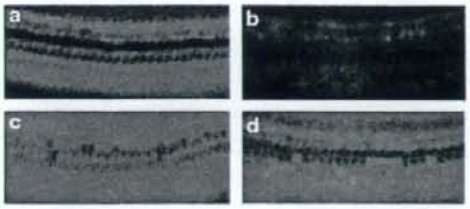

Figure 3 Preservation of the hair cells in the transduced cochlea. Hair cell loss in the cochlea of transduced rats was analyzed by F-actin staining. The dissected samples were dissected from the middle turn of the cochlea. The adeno-asssociated virus 1 (AAV1) vector was injected into the scala tympani of the cochlea prior to 12 days of kanamycin administration. (**a**) The normal cochlea. (**b**) The cochlea from the vehicle-treated ear; the many dark spaces represent the loss of outer hair cells. (**c**) The cochlea from the AAV1-GDNF-transduced ear. (**d**) The cochlea from the contralateral ear of AAV1-GDNF transduced rats. GDNF, glial cell line-derived neurotrophic factor.

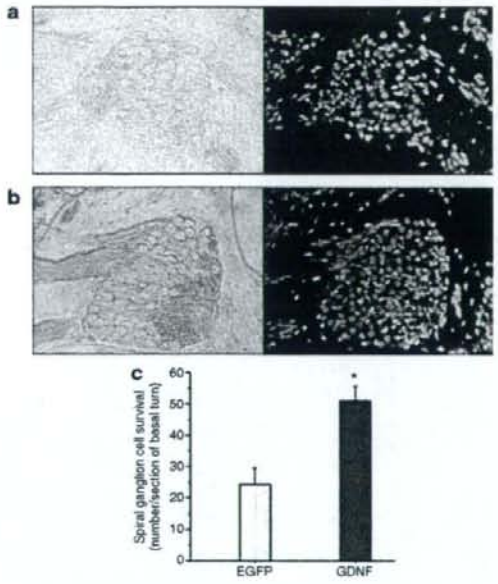

Figure 4 Survival of the spiral ganglion cells in the transduced cochlea. AAV1-GDNF-mediated rescue of the kanamycin-induced damage to the rat spiral ganglion neurons (SGNs): 4′,6-diamino-2-phenylindole dihydrochloride (DAPI) staining was performed on the sections obtained from the rat pretreated with either AAV1-EGFP or AAV1-GDNF, followed by kanamycin injections. (**a**, **b**) Representative photomicrographs of the cryosections showing the basal turn of the cochlear spiral (**a**, AAV1-EGFP; **b**, AAV1-GDNF). (**c**) The number of DAPI-positive large-nucleus cells that exhibited SGN morphology was counted. An asterisk denotes a statistically significant difference between the AAV1-GDNF and AAV1-EGFP-transduced rats (*t*-test, $P < 0.001$). AAV1, adeno-associated virus 1; EGFP, enhanced green fluorescent protein; glial cell line–derived neurotrophic factor.

impairment. At all frequencies tested, both GDNF-transduced and contralateral, untreated ears showed a significant improvement in the threshold shifts compared to the ears transduced with EGFP ($n = 5$, $P < 0.05$) (Figure 5). In the EGFP group, there was

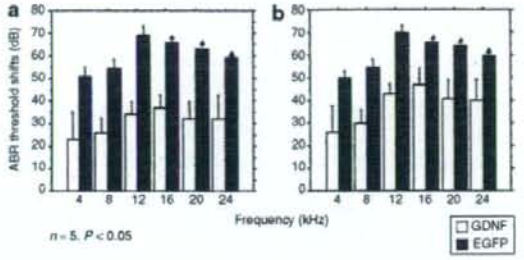

Figure 5 Protection of cochlear function by glial cell line-derived neurotrophic factor GDNF. Auditory brain stem response (ABR) threshold shifts (mean ± SD) of the (**a**) treated and (**b**) untreated ears at each tested frequency in the enhanced green fluorescent protein (EGFP) and GDNF transduced rats. The ABR threshold was measured twice in all the animals. The ears treated with AAV1-GDNF showed a significant improvement in the threshold shifts compared to the ears treated with AAV1-EGFP at all frequencies tested ($n = 5$, $P < 0.05$). Arrows indicate the average ABR thresholds that exceeded the output power of the ABR apparatus. AAV1, adeno-associated virus 1.

no significant difference in the ABR threshold shifts between the transduced and contralateral, untreated cochleae at all frequencies tested. Animals transduced with the AAV1-GDNF demonstrated lower ABR threshold shifts in the injected side compared to the contralateral side (at 12, 16, 20, 24 kHz; $P < 0.05$). These data indicate that both ears were protected even if the AAV1-GDNF was only injected into one ear.

Induced transgene expression

Two hundred and ninety three cells were transduced with the proviral plasmid harboring rtTA2s-S2 and the tetracycline-responsive element (TRE) to express the *EGFP* gene (Figure 1b). In the presence of Dox, a significant level of fluorescence was detected, suggesting that the rtTA2s-S2 system could switch on transcription following Dox treatment (Figure 6a). In contrast, reporter gene expression in the cultured cells was faint in the absence of Dox, indicating a low basal activity *in vitro*. Western blot analysis of GDNF showed that the transgene was induced in the presence of Dox, while no expression was detected in the absence of Dox (Figure 6b).

In vivo induction of GDNF expression and the dose–response to Dox

Enzyme-linked immunosorbent assay analysis of the GDNF expression level in muscle also showed low basal activity and induced expression after Dox treatment (Figure 6c). In the absence of Dox, the expression level of GDNF in the AAV2-S2-GDNF group was as low as that in the phosphate-buffered saline and AAV2-*LacZ* groups. On the other hand, significant increases in the GDNF level were observed in the muscle with increasing amounts of Dox, demonstrating that the rtTA2s-S2 system induces gene expression in a dose-dependent manner.

Inducible GDNF expression in the cochlea

Extensive inducible GDNF transgene expression was confirmed by immunohistochemistry using an anti-FLAG-antibody in the AAV1-S2-GDNF/kanamycin group in the presence of Dox (Figure 7).

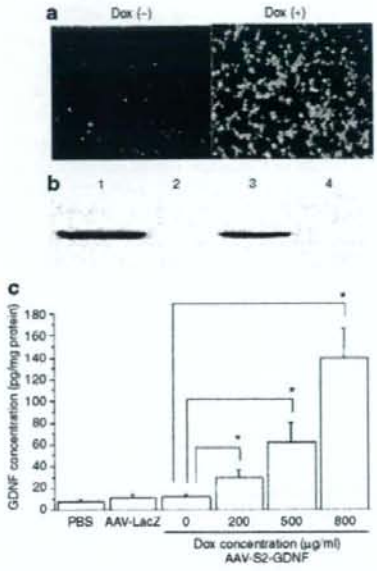

Figure 6 Induction of the transgene expression. (**a**) HEK293 cells were transfected with the proviral plasmid pAAV2-rtTA-S2-TRE-d2EGFP, and the expression of enhanced green fluorescent protein (EGFP) was induced by the doxycycline (Dox) (1 μg/ml). (**b**) Western blot analysis with an anti-FLAG antibody to detect the glial cell line–derived neurotrophic factor (GDNF) expression in the transduced 293 cells with the proviral plasmids. pAAV2-GDNF (lane 1), pAAV2-EGFP (lane 2), pAAV2-rtTA2s-S2-TRE-GDNF with Dox (lane 3), and pAAV2-rtTA2s-S2-TRE-GDNF without Dox (lane 4). (**c**) Dose–response of GDNF in the AAV2-S2-GDNF-injected muscle to the various concentrations of Dox. Mice were injected with phosphate-buffered saline (PBS), AAV2-LacZ, or AAV2-S2-GDNF followed by Dox administered in the drinking water. The mean muscle GDNF concentration in the animals treated with the AAV2-S2-GDNF in the absence of Dox was not significantly different compared to the animals treated with PBS or AAV2-*LacZ* ($P > 0.05$). The GDNF expression levels in the animals transduced with the AAV2-S2-GDNF significantly increased with increasing Dox concentration ($P < 0.05$). AAV1, adeno-associated virus 1.

In contrast, no detectable GDNF expression was observed in the cochlea of the AAV1-S2-GDNF/kanamycin group in the absence of Dox (data not shown).

Protection of cochlear function with induced GDNF expression

To evaluate the adverse effects of the transduction procedure, ABR recordings were performed on kanamycin-free rats after injection of the inducible AAV1-S2-GDNF vectors and Dox administration. At all frequencies tested, no significant increase in the ABR threshold was observed after virus injection (Figure 8a). This result indicates that AAV1 vector injection, transgene expression, and Dox administration did not affect the ABR threshold of the experimental rats. Interestingly, even if AAV1-S2-GDNF was injected into the cochlea of one ear, the cochleas of both ears were protected in the presence of Dox. In particular, the ABR threshold shifts were significantly improved in both the AAV1-S2-GDNF-injected cochlea of the kanamycin-treated rats in the presence of Dox (Figure 8b)

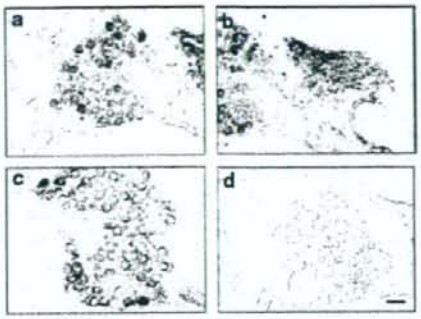

Figure 7 Expression of the GDNFflag in the rat cochlea. (**a**, **b**, **c**) The sections were sampled after the AAV1-S2-GDNF injection into the cochlea in the presence of doxycycline. GDNFflag expression was detected using an anti-FLAG antibody. (**d**) Samples from AAV1-EGFP-inoculated cochlea were analyzed as the negative control. Scale bar = 25 μm; ×400. AAV1, adeno-associated virus 1; GDNF, glial cell line–derived neurotrophic factor; EGFP, enhanced green fluorescent protein.

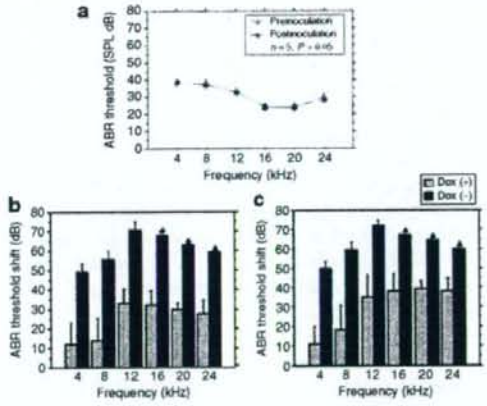

Figure 8 Protection of cochlear function with induced glial cell line–derived neurotrophic factor (GDNF) expression. (**a**) Auditory brain stem response (ABR) thresholds (mean ± SD) at each frequency tested in the AAV1-S2-GDNF-injected rat cochlea in the presence of doxycycline (Dox). No significant difference in the hearing thresholds was observed at each frequency between preinjection and postinjection. SPL, sound pressure level. ABR threshold shifts (mean ± SD) at each tested frequency in the (**b**) transduced or (**c**) nontransduced cochlea with or without Dox. Significant differences in the hearing threshold shifts were observed at each frequency between AAV1-S2-GDNF cochlea in the presence and absence of Dox ($n = 5$, $P < 0.05$). Arrows indicate the average ABR thresholds that exceeded the output power of the ABR apparatus.

and the cochlea of the noninjected contralateral ear (Figure 8c). However, the ABR threshold shifts at all frequencies were significantly lower in the treated group (AAV1-S2-GDNF/kanamycin plus Dox) than in the contralateral, untreated ear.

DISCUSSION

In this study, we showed that both sustained and regulated AAV1-mediated GDNF expression protected the cochlear function of rats from aminoglycoside-induced ototoxicity. Indeed, damaged spiral ganglion cells and hair cells were significantly reduced by

regulated GDNF expression. The ABR monitoring revealed that there was no loss of the cochlear function over the frequencies tested after AAV vector injection and Dox treatment. These data suggest that regulated expression of GDNF in the cochlea efficiently preserves the cochlea from kanamycin-induced ototoxicity.

Among the various viral vector systems, the recombinant AAV-mediated gene transduction system offers several important advantages as a tool for direct somatic gene delivery into the cochlea. These include long-term stable expression of therapeutic genes in a wide variety of postmitotic tissues and minimal vector-related cytotoxicity.[26] In our previous report, we demonstrated the effective transduction of mouse cochleae with the AAV1-based vectors.[7] Generally the therapeutic effectiveness depends on an appropriate concentration and the half-life of the molecules. AAV vector–mediated gene transfer is a promising delivery technique to facilitate a long-term and chronic supply of therapeutic proteins that have a short half-life, such as GDNF. Furthermore, when the CAG promoter is used, efficient transduction activity is observed in the cochlear cells including the inner hair cells and spiral ganglion cells.[27,28]

Our data showed that AAV1-GDNF-mediated transduction of the rat cochleae provided significant protection of the cochlea against aminoglycoside-induced damage. This finding is consistent with previous studies that have used adenovirus-mediated GDNF expression[13,15,16] and demonstrates the feasibility of gene therapy with AAV1-based vectors for drug-induced hearing loss. Although the exact mechanism has not yet been elucidated, antioxidant pathways might be involved in the protective function of GDNF in the inner ear.[29] Free-radical formation following exposure to aminoglycoside is considered one of the major mechanisms to explain the aminoglycoside-related hair cell death.[1,30,31] It has been previously shown that GDNF is endogenously synthesized in the inner hair cells and spiral ganglion cells of the cochlea,[32] and the two known GDNF receptors are present in the spiral ganglion.[17,32,33] In the present study, we inoculated the cochlea with the AAV1 vectors via the round window membrane and detected a high level of transgene expression mainly in the inner hair cells and spiral ganglion cells. The AAV1-mediated GDNF expression pattern was similar to that of the endogenous protein; therefore GDNF supplemented *in situ* can play a substantial role in protection. Although the transduction of the *GDNF* gene was not observed in outer hair cells, GDNF levels in the perilymph of the manipulated cochleae was much higher than in the control cochleae. These cells may respond to the secretion of another growth factor that promotes hair cell survival. Upregulation of GDNF in inner hair cells and spiral ganglion cells following noise also support this concept.[34]

Compared to the vehicle controls, increased cochlear cell survival was observed in the contralateral ears of the AAV1-GDNF group, suggesting that the contralateral cochleae in treated rats were also moderately protected. Expression of the transgene was detected in the contralateral cochlea of the rats after injection with 5×10^{10} genome copies of AAV1 per cochlea (data not shown). AAV can diffuse from one ear to the other via the cerebrospinal fluid in rodents.[35] Therefore, secreted GDNF molecules may also diffuse and exert a protective effect in the opposite ear. Alternatively, GDNF might enhance the neuronal activity (either afferent or efferent) of both ears, protecting both the treated and the contralateral cochlear function. Moreover, since infusion of the vectors into the cochlea forces large amounts of the vectors into the cerebrospinal fluid, any functional effect might be associated with the transduction of the brain. In this context, it is of great interest to know whether the otoprotective effect was achieved by the simple diffusion of the transgene product or direct transduction of the cells in the contralateral ear. To answer this question, we analyzed the local expression of the nonsecretory protein marker in the rodents with this transduction approach. Consequently, we feel that the direct transduction of the cells in the contralateral ear might be involved in the neuroprotection.

The present results showed that AAV-mediated delivery of a Tet-on system was able to control transgene expression. This Tet-on system incorporates the mutant transactivator rtTA2s-S2 and the transgene in which messenger RNA transcription is activated in the presence of an inducer, leading to protein expression. As we showed, the inducible expression of GDNF efficiently protected the cochlear structure and function from kanamycin-induced damage. GDNF was overexpressed in the induced state with the rtTA2s-S2 system, whereas GDNF expression was nearly normal in the non-induced state. In our study, cochlear function was significantly protected from aminoglycoside-induced cochlear damage in the presence of Dox. Although intracochlear injections did not affect physiological cochlear function, intramuscular injections of the vectors expressing Dox-dependent activators may elicit a cellular and humoral response against the transactivator in nonhuman primates.[36–38] The use of tissue-specific promoters that restrict transgene expression to nonprofessional antigen-presenting cells, and the use of AAV vectors, may reduce the induction of a specific T-cell response.[39]

Another attractive feature of the Tet-on system is the high safety profile of the inducer. In our study, Dox was orally administered to the rats to induce GDNF expression. Transgene expression levels were dependent on the dose of Dox, and the dose range of this inducer was below the normal bactericidal treatment levels used in similarly sized animals.[40,41] Furthermore, a Dox regimen in mice that is proportional to a clinically accepted dose of the drug in humans causes a significant induction of transgene expression.

Sequences of antibiotic administration and withdrawal to reverse the Dox induction of therapeutic gene expression were demonstrated in previous studies.[25,42] However, the aminoglycoside-induced hearing impairment model is not an appropriate model for adding and removing the Dox diet because the insulting phase is too short to successively induce and repress the Tet-on system. Furthermore, treatment of age-related hearing loss or genetic hearing loss ideally needs long-term gene expression studies to exclude any adverse events associated with the therapeutic genes.

Efficient control of the tetracycline-regulatory system is based on the specificity of the TetR/tetO interaction and the efficiency and safety of its inducers, such as tetracycline or Dox.[43,44] Mutant tTA2s are composed of one TetR and three repeated oligonucleotides of the VP-16-derived minimal activation domain. In the Tet-on system, rtTA2s-S2 showed a high activating ratio because its background expression level was lower than that of other mutants, such as rtTA2s-M2, which despite having a higher activation potential had also a high initial background.[25] By using the mutant transactivator, Urlinger *et al.* demonstrated that stringent regulation of target genes could be achieved over a range of four to five orders of magnitude

in stably transfected HeLa cells.[24] These regulatory systems could be further optimized to offer several potential advantages. The tetracycline-dependent transcriptional silencer allows tight regulation of transgene expression by eliminating baseline leakage.[20,45] Gene regulation mediated by rtTA2s-S2 was substantially tighter when combined with active silencing by the tetracycline-dependent transcriptional silencer in the non-induced state.[41,46]

Our results show that AAV1-mediated gene transfer is a promising gene delivery approach for the inner ear apparatus. To become an efficient and safe therapeutic method, it will be necessary to improve vector technology to achieve long-term transduction in a fail-safe system. We presented data demonstrating successful AAV-mediated transfer and modulation of transgene expression in the cochlea using a modified Tet-on system. In addition to the need for dosage control of neurotrophic factors, the AAV1 and the Tet-on system maybe useful for the regulation of the expression of other therapeutic gene products in the cochlea. Following further improvements, the rAAV-mediated transduction system may be of potential use for cochlear gene therapy applications in humans.

MATERIALS AND METHODS

Construction and preparation of the plasmids. The AAV vector proviral plasmid pAAV2-CAG-EGFP-WPRE (pAAV2-EGFP) contained the *EGFP* gene under the control of the CAG promoter and the WPRE and was flanked by inverted terminal repeats. A *Bam*HI fragment containing the GDNFflag complementary DNA was subcloned into this plasmid to obtain the pAAV2-CAG-GDNF-WPRE (pAAV2-GDNF) cassette.

The pAAV2-CMV-GDNFflag plasmid with the CMV promoter, the first intron of the human growth hormone gene, and the simian virus 40 polyadenylation signal sequence, were inserted between the inverted terminal repeats of the AAV type 2 genome.[47] The transactivator rtTA2s-S2 complementary DNA in the pUHrT61-1 plasmid (BD Biosciences, San Jose, CA) and the TRE in the pTRE-d2EGFP plasmid (BD Biosciences, CA) were subcloned together into the pAAV2-CMV-GDNFflag plasmid to obtain the AAV vector proviral plasmid pAAV2-rtTA2s-S2-TRE-GDNF. A *Sac*II-*Eco*RI fragment containing the d2EGFP complementary DNA from the pTRE-d2EGFP plasmid (BD Biosciences, CA) was subcloned into this plasmid to create the pAAV2-rtTA2s-S2-TRE-EGFP plasmid (see **Supplementary Materials and Methods**).

Recombinant AAV vector production. The AAV1 vectors were produced as previously described by using a 293-cell transfection protocol[26] with the proviral plasmid pAAV2-EGFP, pAAV2-Luciferase,[48] pAAV2-GDNF, pAAV2-rtTA2s-S2-TRE-EGFP, or pAAV2-rtTA2s-S2-TRE-GDNF; the AAV packaging plasmid pAAV1RepCap; and the adenovirus helper plasmid pAdeno5 using an active gassing system.[49] The recombinant AAV2 expressing the *Escherichia coli* β-galactosidase gene under the control of the CMV promoter (AAV2-LacZ) was generated using the proviral plasmid pAAV-LacZ.[50] (see **Supplementary Materials and Methods**).

In vitro expression of GDNF. To detect the *in vitro* expression of the GDNFflag fusion protein, 293 cells were transduced with the AAV1-GDNFflag at 1×10^4 vector genome copies/cell. For the detection of the regulated expression, 293 cells were transduced with the AAV proviral plasmid pAAV2-rtTA2s-S2-TRE-d2EGFP or pAAV2-rtTA2s-S2-TRE-GDNF in the presence or absence of 1 μmol/l Dox-HCl (Sigma, St Louis, MO) (see **Supplementary Materials and Methods**).

Surgical procedures and cochlear perfusions. All animal studies were performed in accordance with the guidelines issued by the committee on animal research at Jichi Medical University. Twenty 5-week-old male Sprague–Dawley rats with normal Preyer's reflexes weighing 130–150 g were utilized (CLEA Japan, Tokyo, Japan). Five-week-old male C57BL/6J mice were utilized for optical bioluminescence imaging. The animals were anesthetized with ketamine (50 mg/kg) and xylazine (5 mg/kg). A post-auricular approach was performed to expose the tympanic bony bulla. A small opening (2 mm in diameter) to the tympanic bulla was made by carefully drilling through the bone of the bulla to gain access to the round window membrane. Subsequently, 5 μl of AAV vector solution (AAV1-EGFP, AAV2-Luciferase, or AAV1-GDNF, 5×10^{10} genome copies, $n = 5$ each) was microinjected into the cochlea through the round window for over 10 minutes using a glass micropipette (40 μm in diameter) fitted on a Univentor 801 syringe pump (Serial No. 170182, High Precision Instruments, Univentor Ltd., Malta). The rats were also injected with the AAV1-S2-GDNF in the presence ($n = 5$) or absence ($n = 5$) of Dox. A small plug of muscle was used to seal the cochlea, and the surgical wound was closed in layers and dressed with an antibiotic ointment.

Transgene expression in vivo. The rats were deeply anesthetized and the perilymph was sampled from the inoculated cochlea through the round window. GDNF protein levels were measured using a GDNF Emax ImmunoAssay System (Promega, Madison, WI) according to the manufacturer's instructions. The GDNF expression in the rat cochlea was determined by immunohistochemistry using an anti-FLAG antibody.

AAV2-LacZ or AAV2-S2-GDNF vector (1×10^{10} genome copies) was injected into the quadriceps of the C57BL/6J mice (6 weeks old, CLEA Japan, Tokyo, Japan). The mice were injected with phosphate-buffered saline ($n = 5$) or AAV2-*LacZ* ($n = 5$). Animals treated with various concentrations of Dox were injected with the AAV2-S2-GDNF ($n = 5$ per group). Two weeks after the transduction, animals were deeply anesthetized, and the injected muscle was sampled. The tissue levels of the GDNF protein were measured with an enzyme-linked immunosorbent assay kit (GDNF Emax ImmunoAssay System, Promega, WI), according to the manufacturer's instructions. The levels of GDNF were expressed as pg/mg protein. The assay sensitivity ranged from 16 to 1,000 pg/ml.

Two weeks after the injection of the AAV2-Luciferase, optical bioluminescence imaging was performed using the CCD camera (Xenogen, Alameda, CA). After intraperitoneal injection of reporter substrate D-Luciferin (375 mg/kg body weight), mice were imaged for scans.

Kanamycin administration and ABR assessment. A dose of 333 mg of kanamycin base/kg body weight was obtained by injecting 3 μl/g body weight. Seven days after virus injection, kanamycin was given subcutaneously twice daily for 12 consecutive days. The body weight of the animals was monitored daily to adjust the kanamycin dosages accordingly.

Auditory thresholds were determined by audiometry of evoked ABRs using Tucker-DAVIS Technologies and Scope software (Power Lab; ADInstruments, Colorado Springs, CO). Thresholds were evaluated for each animal prior to the start of the injection procedure and 2 days after the termination of kanamycin treatment. The ABRs were measured as previously described,[7] using a two-way repeated analysis of variance (see **Supplementary Materials and Methods**).

Histological evaluation of the cochlear preservation. Cochlear hair cell loss was determined by F-actin staining. One month after transduction, the presence of the cochlear spiral ganglion neurons was determined by 4′,6-diamino-2-phenylindole dihydrochloride staining to visualize nuclear chromatin. After decalcification, 6 μm mid-modiolus cryosections of the cochleae from each animal were histologically analyzed. The number of spiral ganglion neurons was determined in every third section of the cochlear basal turn from the AAV1-transduced and kanamycin-treated rats (see **Supplementary Materials and Methods**).

Statistical analyses. Results are presented as the means ± SD. Data were statistically analyzed using analysis of variance, paired student's *t*-test (injected versus contralateral sides) or unpaired student's *t*-test (therapy versus control groups) (StatView 5.0 software; SAS Institute, Cary, NC).

ACKNOWLEDGMENTS

The authors thank Avigen. (Alameda, CA) for providing the pAAV-LacZ and pAdeno. We also thank Thomas Hope (Department of Microbiology and Immunology, The University of Illinois at Chicago) for providing pBS II SK+WPRE-B11 and Jun-Ichi Miyazaki (Osaka University Graduate School of Medicine, Osaka, Japan) for pCAGGS. The authors also thank Miyoko Mitsu for her encouragement and technical support. This work was supported in part by grants from the Ministry of Health, Labour and Welfare of Japan (Grants-in-Aid for Scientific Research and grant for 21 Century Centers of Excellence program) and the "High-Tech Research Center" Project for Private Universities (matching fund subsidy, from the Ministry of Education, Culture, Sports, Science, and Technology of Japan). The authors declare no conflict of interest.

SUPPLEMENTARY MATERIAL

Materials and Methods.

Figure S1. Bioluminescence of the transduced cochlea in living mice.

REFERENCES

1. Wu, WJ, Sha, SH and Schacht, J (2002). Recent advances in understanding aminoglycoside ototoxicity and its prevention. *Audiol Neurootol* **7**: 171–174.
2. Hellier, WP, Wagstaff, SA, O'Leary, SJ and Shepherd, RK (2002). Functional and morphological response of the stria vascularis following a sensorineural hearing loss. *Hear Res* **172**: 127–136.
3. Tsue, TT, Oesterle, EC and Rubel, EW (1994). Hair cell regeneration in the inner ear. *Otolaryngol Head Neck Surg* **111**: 281–301.
4. Raphael, Y, Frisancho, JC and Roessler, BJ (1996). Adenoviral-mediated gene transfer into guinea pig cochlear cells *in vivo*. *Neurosci Lett* **207**: 137–141.
5. Ishimoto, S, Kawamoto, K, Kanzaki, S and Raphael, Y (2002). Gene transfer into supporting cells of the organ of Corti. *Hear Res* **173**: 187–197.
6. Okada, T, Nomoto, T, Shimazaki, K, Lijun, W, Lu, Y, Matsushita, T *et al.* (2002). Adeno-associated virus vectors for gene transfer to the brain. *Methods* **28**: 237–247.
7. Liu, Y, Okada, T, Sheykholeslami, K, Shimazaki, K, Nomoto, T, Muramatsu, SI *et al.* (2005). Specific and efficient transduction of cochlear inner hair cells with recombinant adeno-associated virus type 3 vector. *Mol Ther* **12**: 725–733.
8. Lin, LF, Doherty, DH, Lile, JD, Bektesh, S and Collins, F (1993). GDNF: a glial cell line-derived neurotrophic factor for midbrain dopaminergic neurons. *Science* **260**: 1130–1132.
9. Henderson, CE, Phillips, HS, Pollock, RA, Davies, AM, Lemeulle, C, Armanini, M *et al.* (1994). GDNF: a potent survival factor for motoneurons present in peripheral nerve and muscle. *Science* **266**: 1062–1064.
10. Wang, Y, Lin, SZ, Chiou, AL, Williams, LR and Hoffer, BJ (1997). Glial cell line-derived neurotrophic factor protects against ischemia-induced injury in the cerebral cortex. *J Neurosci* **17**: 4341–4348.
11. Keithley, EM, Ma, CL, Ryan, AF, Louis, JC and Magal, E (1998). GDNF protects the cochlea against noise damage. *Neuroreport* **9**: 2183–2187.
12. Shoji, F, Yamasoba, T, Magal, E, Dolan, DF, Altschuler, RA and Miller, JM (2000). Glial cell line-derived neurotrophic factor has a dose-dependent influence on noise-induced hearing loss in the guinea pig cochlea. *Hear Res* **142**: 41–55.
13. Suzuki, M, Yagi, M, Brown, JN, Miller, AL, Miller, JM and Raphael, Y (2000). Effect of transgenic GDNF expression on gentamicin-induced cochlear and vestibular toxicity. *Gene Ther* **7**: 1046–1054.
14. Yagi, M, Kanzaki, S, Kawamoto, K, Shin, B, Shah, PP, Magal, E *et al.* (2000). Spiral ganglion neurons are protected from degeneration by GDNF gene therapy. *J Assoc Res Otolaryngol* **1**: 315–325.
15. Hakuba, N, Watabe, K, Hyodo, J, Ohashi, T, Eto, Y, Taniguchi, M *et al.* (2003). Adenovirus-mediated overexpression of a gene prevents hearing loss and progressive inner hair cell loss after transient cochlear ischemia in gerbils. *Gene Ther* **10**: 426–433.
16. Kawamoto, K, Yagi, M, Stover, T, Kanzaki, S and Raphael, Y (2003). Hearing and hair cells are protected by adenoviral gene therapy with TGF-beta1 and GDNF. *Mol Ther* **7**: 484–492.
17. Kuang, R, Hever, G, Zajic, G, Yan, Q, Collins, F, Louis, JC *et al.* (1999). Glial cell line-derived neurotrophic factor. Potential for otoprotection. *Ann NY Acad Sci* **884**: 270–291.
18. Yagi, M, Magal, E, Sheng, Z, Ang, KA and Raphael, Y (1999). Hair cell protection from aminoglycoside ototoxicity by adenovirus-mediated overexpression of glial cell line-derived neurotrophic factor. *Hum Gene Ther* **10**: 813–823.
19. Meng, X, Lindahl, M, Hyvonen, ME, Parvinen, M, de Rooij, DG, Hess, MW *et al.* (2000). Regulation of cell fate decision of undifferentiated spermatogonia by GDNF. *Science* **287**: 1489–1493.
20. Perez, N, Plenge, P, Millet, V, Greuet, D, Minot, C, Noel, D *et al.* (2002). Tetracycline transcriptional silencer tightly controls transgene expression after *in vivo* intramuscular electrotransfer: application to interleukin 10 therapy in experimental arthritis. *Hum Gene Ther* **13**: 2161–2172.
21. Regulier, E, Pereira de Almeida, L, Sommer, B, Aebischer, P and Deglon, N (2002). Dose-dependent neuroprotective effect of ciliary neurotrophic factor delivered via tetracycline-regulated lentiviral vectors in the quinolinic acid rat model of Huntington's disease. *Hum Gene Ther* **13**: 1981–1990.
22. Rubinchik, S, Worarataanadharm, J, Yu, H and Dong, JY (2005). New complex Ad vectors incorporating both rtTA and tTS deliver tightly regulated transgene expression both *in vitro* and *in vivo*. *Gene Ther* **12**: 504–511.
23. Pluta, K, Luce, MJ, Bao, L, Agha-Mohammadi, S and Reiser, J (2005). Tight control of transgene expression by lentivirus vectors containing second-generation tetracycline-responsive promoters. *J Gene Med* **7**: 803–817.
24. Urlinger, S, Baron, U, Thellmann, M, Hasan, MT, Bujard, H and Hillen, W (2000). Exploring the sequence space for tetracycline-dependent transcriptional activators: novel mutations yield expanded range and sensitivity. *Proc Natl Acad Sci USA* **97**: 7963–7968.
25. Lamartina, S, Roscilli, G, Rinaudo, CD, Sponeno, E, Silvi, L, Hillen, W *et al.* (2002). Stringent control of gene expression *in vivo* by using novel doxycycline-dependent trans-activators. *Hum Gene Ther* **13**: 199–210.
26. Okada, T, Shimazaki, K, Nomoto, T, Matsushita, T, Mizukami, H, Urabe, M *et al.* (2002). Adeno-associated viral vector-mediated gene therapy of ischemia-induced neuronal death. *Methods Enzymol* **346**: 378–393.
27. Stone, IM, Lurie, DI, Kelley, MW and Poulsen, DJ (2005). Adeno-associated virus-mediated gene transfer to hair cells and support cells of the murine cochlea. *Mol Ther* **11**: 843–848.
28. Liu, Y, Okada, T, Nomoto, T, Ke, X, Kume, A, Ozawa, K *et al.* (2007). Promoter effects of adeno-associated viral vector for transgene expression in the cochlea *in vivo*. *Exp Mol Med* **39**: 170–175.
29. Oppenheim, RW (1997). Related mechanisms of action of growth factors and antioxidants in apoptosis: an overview. *Adv Neurol* **72**: 69–78.
30. Priuska, EM and Schacht, J (1995). Formation of free radicals by gentamicin and iron and evidence for an iron/gentamicin complex. *Biochem Pharmacol* **50**: 1749–1752.
31. Sha, SH and Schacht, J (1999). Stimulation of free radical formation by aminoglycoside antibiotics. *Hear Res* **128**: 112–118.
32. Sanikola, M, Hession, C, Worley, D, Carmillo, P, Ehrenfels, C, Walus, L *et al.* (1997). Glial cell line-derived neurotrophic factor-dependent RET activation can be mediated by two different cell-surface accessory proteins. *Proc Natl Acad Sci USA* **94**: 6238–6243.
33. Ylikoski, J, Pirvola, U, Virkkala, J, Suvanto, P, Liang, XQ, Magal, E *et al.* (1998). Guinea pig auditory neurons are protected by glial cell line-derived growth factor from degeneration after noise trauma. *Hear Res* **124**: 17–26.
34. Nam, YJ, Stover, T, Hartman, SS and Altschuler, RA (2000). Upregulation of glial cell line-derived neurotrophic factor (GDNF) in the rat cochlea following noise. *Hear Res* **146**: 1–6.
35. Kho, ST, Pettis, RM, Mhatre, AN and Lalwani, AK (2000). Safety of adeno-associated virus as cochlear gene transfer vector: analysis of distant spread beyond injected cochlea. *Mol Ther* **2**: 368–373.
36. Favre, D, Blouin, V, Provost, N, Spisek, R, Porrot, F, Bohl, D *et al.* (2002). Lack of an immune response against the tetracycline-dependent transactivator correlates with long-term doxycycline-regulated transgene expression in non-human primates after intramuscular injection of recombinant adeno-associated virus. *J Virol* **76**: 11605–11611.
37. Latta-Mahieu, M, Rolland, M, Caillet, C, Wang, M, Kennel, P, Mahfouz, I *et al.* (2002). Gene transfer of a chimeric trans-activator is immunogenic and results in short-lived transgene expression. *Hum Gene Ther* **13**: 1611–1620.
38. Lena, AM, Giannetti, P, Sporeno, E, Ciliberto, G and Savino, R (2005). Immune responses against tetracycline-dependent transactivators affect long-term expression of mouse erythropoietin delivered by a helper-dependent adenoviral vector. *J Gene Med* **7**: 1086–1096.
39. Cordier, L, Gao, GP, Hack, AA, McNally, EM, Wilson, JM, Chirmule, N *et al.* (2001). Muscle-specific promoters may be necessary for adeno-associated virus-mediated gene transfer in the treatment of muscular dystrophies. *Hum Gene Ther* **12**: 205–215.
40. McGee Sanftner, LH, Rendahl, KG, Quiroz, D, Coyne, M, Ladner, M, Manning, WC *et al.* (2001). Recombinant AAV-mediated delivery of a tet-inducible reporter gene to the rat retina. *Mol Ther* **3**: 688–696.
41. Lamartina, S, Silvi, L, Roscilli, G, Casimiro, D, Simon, AJ, Davies, ME *et al.* (2003). Construction of an rtTA2(s)-m2/tts(kid)-based transcription regulatory switch that displays no basal activity, good inducibility, and high responsiveness to doxycycline in mice and non-human primates. *Mol Ther* **7**: 271–280.
42. Srour, MA, Fechner, H, Wang, X, Siemetzki, U, Albert, T, Oldenburg, J *et al.* (2003). Regulation of human factor IX expression using doxycycline-inducible gene expression system. *Thromb Haemost* **90**: 398–405.
43. Kistner, A, Gossen, M, Zimmermann, F, Jerecic, J, Ullmer, C, Lubbert, H *et al.* (1996). Doxycycline-mediated quantitative and tissue-specific control of gene expression in transgenic mice. *Proc Natl Acad Sci USA* **93**: 10933–10938.
44. Knott, A, Garke, K, Urlinger, S, Guthmann, J, Muller, Y, Thellmann, M *et al.* (2002). Tetracycline-dependent gene regulation: combinations of transregulators yield a variety of expression windows. *Biotechniques* **32**: 796, 798, 800 passim.
45. Rendahl, KG, Quiroz, D, Ladner, M, Coyne, M, Seltzer, J, Manning, WC *et al.* (2002). Tightly regulated long-term erythropoietin expression in vivo using tet-inducible recombinant adeno-associated viral vectors. *Hum Gene Ther* **13**: 335–342.
46. Salucci, V, Scarito, A, Aurisicchio, L, Lamartina, S, Nicolaus, G, Giampaoli, S *et al.* (2002). Tight control of gene expression by a helper-dependent adenovirus vector carrying the rtTA2(s)-M2 tetracycline transactivator and repressor system. *Gene Ther* **9**: 1415–1421.
47. Wang, L, Muramatsu, S, Lu, Y, Ikeguchi, K, Fujimoto, K, Okada, T *et al.* (2002). Delayed delivery of AAV-GDNF prevents nigral neurodegeneration and promotes functional recovery in a rat model of Parkinson's disease. *Gene Ther* **9**: 381–389.
48. Okada, T, Uchibori, R, Iwata-Okada, M, Takahashi, M, Nomoto, T, Nonaka-Sarukawa, M *et al.* (2006). A histone deacetylase inhibitor enhances recombinant adeno-associated virus-mediated gene expression in tumor cells. *Mol Ther* **13**: 738–746.
49. Okada, T, Nomoto, T, Yoshioka, T, Nonaka-Sarukawa, M, Ito, T, Ogura, T *et al.* (2005). Large-scale production of recombinant viruses by use of a large culture-vessel with active gassing. *Hum Gene Ther* **16**: 1212–1218.
50. Okada, T, Mizukami, H, Urabe, M, Nomoto, T, Matsushita, T, Hanazono, Y *et al.* (2001). Development and characterization of an antisense-mediated prepackaging cell line for adeno-associated virus vector production. *Biochem Biophys Res Commun* **288**: 62–68.

Therapeutic Effects of Hepatocyte Transplantation on Hemophilia B

Kohei Tatsumi,[1] Kazuo Ohashi,[2,3,4,5] Midori Shima,[1] Yoshiyuki Nakajima,[2] Teruo Okano,[3] and Akira Yoshioka[1]

Hepatocyte transplantation offers an alternative therapeutic approach in the treatment of liver-related diseases. Hemophilia B is a bleeding disorder lacking factor IX (FIX) production in the liver, and achieving more than 1% coagulation activity results in significant improvement in the quality of life of the patients. The aim of this study was to investigate the efficacy of hepatocyte transplantation in the mouse model of hemophilia B. We transplanted isolated normal mouse hepatocytes into the liver of FIX knock-out mice. In some recipient mice, additional hepatocyte transplantations were performed 15 days after the first transplant. The recipient plasma FIX activities increased at 1% to 2% and persisted throughout the experimental period. An additional increase was achieved by the repeated transplantation. Close correlation between FIX messenger RNA levels of the liver and plasma FIX activity levels was observed. These results demonstrate that hepatocyte transplantation can provide therapeutic benefits in the treatment of hemophilia B.

Keywords: Hepatocyte transplantation, Hemophilia B, Coagulation factor IX, Experimental transplantation.

(*Transplantation* 2008;86: 167–170)

Hemophilia B, a recessive X-chromosome linked congenital bleeding disorder, is caused by a failure in the production of coagulation factor IX (FIX) (*1*). The only treatments that are currently available are the replacement therapy with FIX concentrates from plasma-derived or recombinant protein sources (*2*). This treatment modality is inefficient and expensive, because of the requirement of life-long and frequent intravenous infusion of FIX concentrates. Although the gene therapy has been actively studied over the past decade to establish a novel therapy that could provide longer acting and safer production of FIX (3), recent clinical trials have yet to conclusively shown long-term therapeutic benefits (*4*, 5). One potential approach that may provide the FIX producing ability in hemophilia B is a whole liver transplantation, because FIX is predominantly produced in the liver (*6–8*). However, the establishment of organ transplantation as a common therapy is hampered by a worldwide shortage of donor livers. Provided that some portion of the donated liver can be used for the isolation of individual hepatocytes, this donor shortage would no longer be a major issue. This is an important point, because the cell type responsible for synthesizing coagulation FIX is the hepatocyte (*9*). Therefore, a cell-based therapy using isolated hepatocytes could provide a therapeutic approach in the treatment of hemophilia B. Hepatocyte transplantation has been recently performed in several countries for various inherited disorders of hepatic metabolism and acute liver failure (*10, 11*). In bleeding disorder, hepatocyte transplantation was applied in the clinics by Dhawan et al. (*12*), who described therapeutic benefits in two patients suffering with congenital factor VII deficiency. Our group has recently shown applying a tissue engineering approach using primary hepatocytes could successfully provide therapeutic effects in hemophilia A mice (*13*). However, the effect of hepatocyte transplantation to treat hemophilia B has yet to be experimentally documented in animals or in the clinics to the best of our knowledge. For this reason, this study was designed to investigate the efficacy of hepatocyte transplantation on hemophilia B.

Hepatocytes were isolated from C57Bl/6 wild-type mice using a collagenase perfusion method as previously described (*13–16*). The recipient FIX knock-out (FIX-KO) mice, syngeneic to donor mice (*17*), were transplanted with the isolated hepatocytes (1.5×10^6 cells in 200 μL) into the liver through the inferior pole of the spleen (n=25). As an experimental control, several FIX-KO mice received sham operation (n=7). To avoid excessive surgical procedure-related bleeding, all FIX-KO mice received intraperitoneal injection of 0.5 mL pooled normal mouse plasma 30 min before abdominal surgery (*18*). All procedures were successfully carried out without any issues related to bleeding and all of the mice survived throughout the experimental period. At days 5, 10, and 15, some of the mice were killed for histologic and messenger RNA (mRNA) analyses (n=7, 5, and 4, at each time point, respectively). All sham-operated mice were killed at day 15.

Blood samples were periodically obtained from retro-orbital plexus of the experimental mice. After anticoagulated with 0.1 volume of 3.8% sodium citrate, blood samples were centrifuged, and plasma samples were stored at −80°C until being analyzed. The plasma FIX activity (FIX:C) was quanti-

This work was supported by grants form AIDS Research from the Ministry of Health, Labor and Welfare of Japan (A.Y.) and grant-in-Aid (18591957) (K.O.) and Special Coordination Funds for Promoting Science and Technology (K.O., T.O.), and from the Ministry of Education, Culture, Sports, Science and Technology (MEXT), Japan.

[1] Department of Pediatrics, Nara Medical University, Kashihara, Nara, Japan.
[2] Department of Surgery, Nara Medical University, Kashihara, Nara, Japan.
[3] Institute of Advanced Biomedical Engineering and Science, Tokyo Women's Medical University, Shinjuku-ku, Tokyo, Japan.
[4] Department of Gastroenterological Surgery Tokyo Women's Medical University, Tokyo, Japan.
[5] Address correspondence to: Kazuo Ohashi, M.D., Ph.D., Institute of Advanced Biomedical Engineering and Science, Tokyo Women's Medical University, 8-1 Kawada-cho, Shinjuku-ku, Tokyo 162-8666, Japan.
E-mail: ohashi@abmes.twmu.ac.jp

Received 8 November 2007. Revision requested 11 December 2007.
Accepted 2 April 2008.

ISSN 0041-1337/08/8601-167
DOI: 10.1097/TP.0b013e31817b9160